Characterizing Crown Biomass and Crown Profiles in Conifer Forests of the Interior Northwest

Final Report: JFSP Project No. 10-1-02-13

Principal Investigators

Dr. David Affleck	Dept. Forest Management, University of Montana
Dr. Carl Seielstad	Dept. Forest Management, University of Montana
Dr. John Goodburn	Dept. Forest Management, University of Montana
Dr. LLoyd Queen	Dept. Forest Management, University of Montana

Federal Cooperator

Dr. Robert Keane	Rocky Mountain Research Station, USDA Forest Service

Table of Contents

1 Abstract

Detailed and accurate models of conifer crown biomass and its distribution are needed for a range of forest management and planning applications, ranging from fuels treatment designs to forest carbon inventory and monitoring. This project focused on the development and integration of novel data collection strategies and analytical methods to better inform crown biomass and fuels estimation for coniferous forests in the interior northwest. Crown biomass data were collected for 7 important conifer species across the interior northwest using randomized branch sampling strategies, and terrestrial laser scanning was used to characterize crown profiles and internal heterogeneity. Results highlight (1) the crucial importance of collecting biomass and fuels data from large diameter trees; (2) the need to consider sampling error in validation of biomass equations; (3) the importance of height and crown length dimensions in prediction of crown biomass; (4) the non-geometric and species-specific character of conifer crown profiles; and (5) the non-uniform distribution of fuels within the crown envelope.

2 Background & Purpose

Active management of large areas of public and private coniferous forest in the western USA is increasingly being shaped by wildfire hazard mitigation, bio-energy development, and carbon sequestration interests. Each of these interests demands credible quantitative descriptions of tree crown and forest canopy architecture. At the tree-level, crowns condition light interception and evapotranspiration, making them key components of ecosystem productivity and drivers forest biomass accumulation. Scaling up to the stand-level, the ability to estimate crown biomass per unit area and crown connectivity becomes critical for modeling fuels and potential fire behavior, for predicting stand growth, and for understanding allocations of aboveground biomass and carbon.

This project was developed to address a 2010 Request for Applications for research on conifer canopy fuels estimation. It represents an effort to develop and integrate novel data collection strategies and analytical methods to better inform crown biomass estimation and fuels management for coniferous forests in the interior northwest. Within this region the crown biomass equations developed by Brown (1978) have been broadly applied to estimate crown fuels while the national-level biomass estimators reported by Jenkins et al. (2003) have been utilized in forest inventory applications. Yet with heightened interest in forest fuels, biomass, and carbon estimation the accuracy of these equations sets has been questioned (e.g., Zhou and Hemstrom 2009). Additionally, recent work has highlighted the importance of the vertical distribution of crown biomass in conditioning wildfire behavior (Keyser & Smith 2009; Parsons et al. 2011), yet there has been little research within the region providing information on the spatial structure of the crowns of interior coniferous species.

The specific aims of the project were to evaluate and describe crown mass allometries for the most important conifer species of the interior northwest using destructive sampling methods as well as to characterize crown structural elements using ground-based remote sensing. These aims were realized through four project objectives:

1) Develop and apply accurate and efficient crown sampling strategies to collect new biomass data for important conifer species from across the interior northwest;
2) Develop a statistical validation methodology to evaluate the performance of existing crown biomass equations utilized in the interior northwest;
3) Evaluate the importance of stem and crown metrics as predictors of crown biomass and advance new crown mass equations for interior northwest species;
4) Investigate the potential of terrestrial laser scanning data collection and processing technology for characterizing crown profiles and structure.

3 Study Description & Location

The study employed two distinct methodological approaches: destructive randomized branch sampling (RBS) for crown biomass estimation and terrestrial laser scanning (TLS) for crown profile delineation. Although undertaken jointly and at an overlapping set of field locations in the interior northwest, these methods yielded data requiring distinct processing and analytical techniques.

3.1 Tree Biomass Data Collection & Analysis

3.1.1 Sampling Methodology & Distribution

Stand and tree selection

Data collection efforts were focused on seven species: Douglas-fir (DF: *Pseudotsuga menziesii*), ponderosa pine (PP: *Pinus ponderosa*), lodgepole pine (PL: *Pinus contorta*), western larch (WL: *Larix occidentalis*), Engelmann spruce (ES: *Picea engelmannii*), grand fir (GF: *Abies grandis*), and subalpine fir (SF: *Abies lasiocarpa*). Stands were selected purposefully with the assistance of federal, state, tribal, or private land managers, whose permission to destructively sample trees from their lands had been obtained. These stands were selected so as to ensure trees of each species and of varying DBH were sampled across the range of habitat types and elevations where they commonly occur. The geographic distribution of sample stands is shown in Fig. 3-1.

Once stands were selected, sample points were established on a systematic grid using the UTM coordinate system. When a sample point was located, an angle gauge was used to identify candidate trees for destructive sampling. At each point, a maximum of two candidate trees were selected for destructive sampling. A tree was removed from the pool of candidates if i) its species was not one of the 7 species of interest, ii) the crown was broken, damaged, or had multiple tops, iii) the crown exhibited excessive signs of insect or disease damage, or iv) the tree could not be felled safely. Furthermore, as sampling progressed, selection preference was given to trees in species × diameter classes where data were sparse.

Tree measurements

When suitable sample trees had been identified, destructive sampling commenced. Measures of DBH, total height, height to the base of the live crown, and crown ratio were taken prior to felling. Crown breakage was minimized by directionally felling the tree into an area large enough to accommodate the crown. When the tree was on the ground, a reel tape was attached at breast height and run along the length of the bole to the tip. Between 5 and 10 live branches were then selected from the crown of each tree using randomized branch sampling (RBS; Gregoire & Valentine 2008). RBS was initiated at the height of the lowest live branch and proceeded up the bole in one meter intervals until either the last sample branch was selected or the bole tapered to a diameter of 5 cm (the tip was treated as a branch and as part of the

crown). Branches were selected within the one meter intervals randomly with probability proportional to branch basal area (as measured outside bark with calipers). An outside bark measure of stem area at the top of each one meter segment was used as a surrogate measure for the aggregate branch basal area positioned in the crown above the current section (see Schlecht & Affleck 2013). Selected live branches were immediately separated by fuel size class, bagged, and labeled. Dead and epicormic branches were weighed (green) in aggregate for each section, with a subsample being retained for drying and weighing.

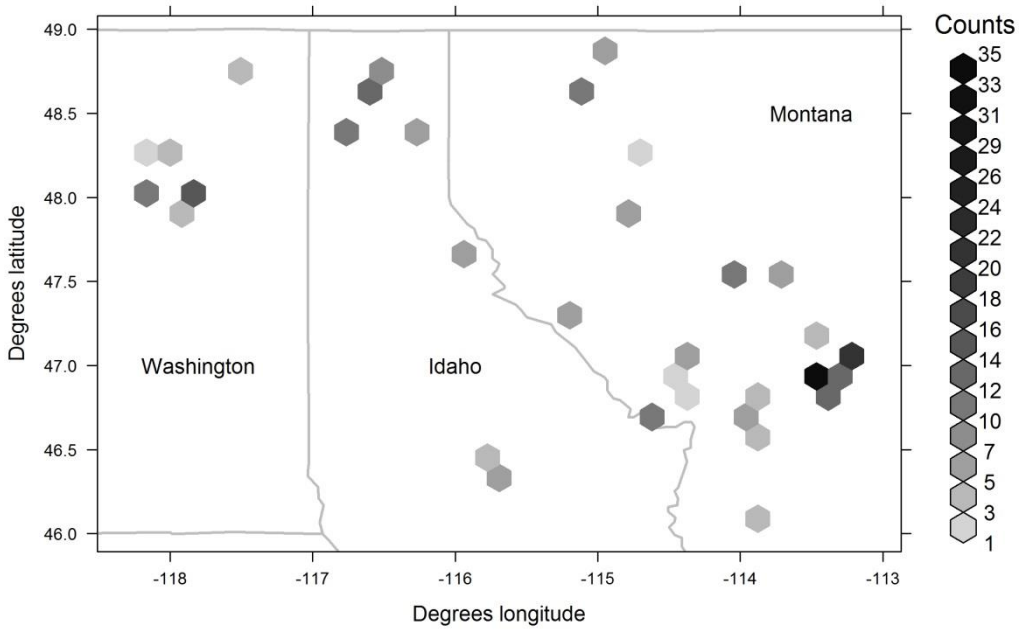

Figure 3-1. Geographic distribution of destructively sampled trees across the interior northwest; legend at right indexes number of trees per hexagon.

Once all branches had been measured and separated from the bole, three locations along the bole were identified for disc extraction. When possible, disc locations were determined in a systematic random fashion such that distance between disc locations was one third of the length of the stem, with the position of the first disc being determined randomly. If sample trees were obtained from an area with active timber management, the disc locations were selected so as to allow sawlogs of prescribed merchantable lengths to be retained.

Laboratory Procedures

Sample materials collected in the field (branches and discs) were subsequently processed in the laboratory. Live branch samples were separated into foliage, 1-hour branchwood (diameter below 0.625 cm), 10-hour branchwood (diameter between 0.625 cm and 2.5 cm), and 100+-hour branchwood (diameter above 2.5 cm). Once separated, these components and the sample discs were dried in forced-air ovens at a temperature of 105°C until a constant weight was reached. Component dry weights were then combined with RBS unconditional branch

selection probabilities to generate crown-level estimates. Since epicormic and dead branches were weighed in aggregate in the field, the ratio of dry to green weight from the sample portions was applied to the aggregate green weights to estimate these components' contributions to whole crown biomass.

Sample Distribution

The distribution of sample trees by DBH, total height (H), and crown length (CL) is given in Table 3-1, and depicted for PP and DF in Fig. 3-2. Distributions for all 7 species are shown in Appendix B. Sample sizes for ES, GF, and SF were smaller than for other species because of i) difficulties encountered in locating and accessing terrain with these species (especially ES and SF), and ii) the fact that crown sampling is typically more time-intensive for these species owing to their long and heavily branched crowns. Yet for each of the target species, trees spanning wide ranges of DBH were obtained with appreciable variations in CL across those ranges. An exception is that for PL no large sample trees (i.e., DBH>30 cm or H>20 m) with crown ratios exceeding 60% were obtained.

.

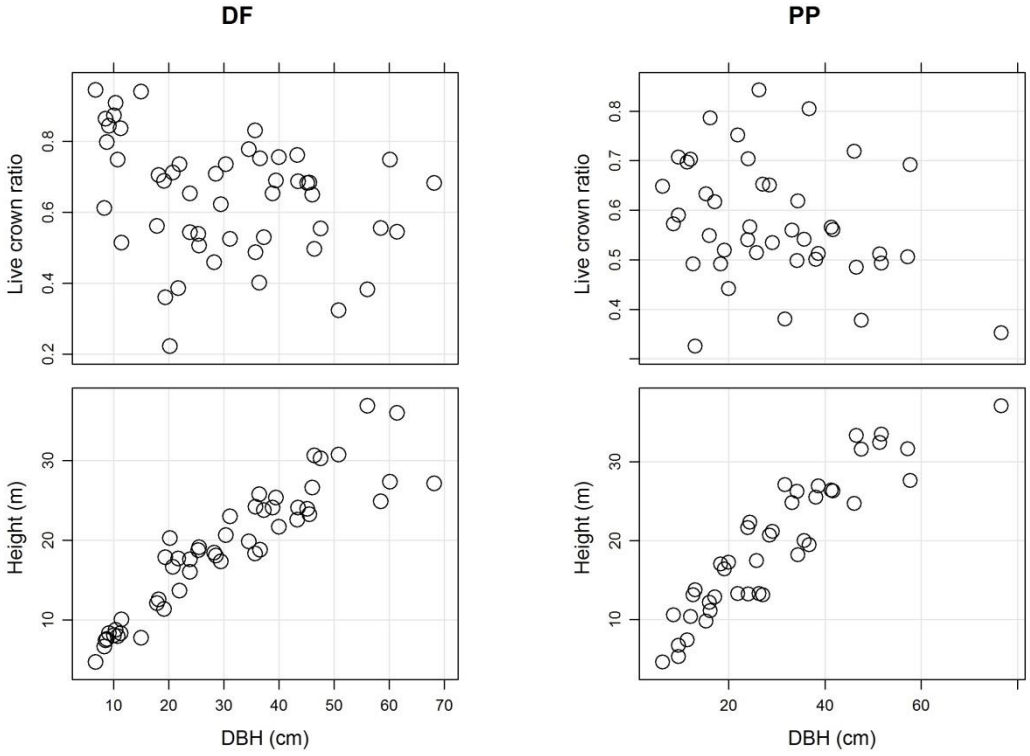

Figure 3-2. DBH, height, and crown ratio distribution of destructively sampled DF and PP.

Table 3-1. Distribution of destructively sampled trees by species.

Species	Num. trees	Num. stands	Mean DBH (cm)	Mean height (m)	Mean crown ratio (%)
DF	46	21	29.5	18.2	65.0
WL	37	10	26.2	20.3	56.1
PP	42	10	29.4	19.5	57.6
PL	39	14	25.4	19.7	47.9
GF	35	9	21.1	16.9	70.1
SF	36	12	20.7	14.6	81.7
ES	34	11	23.2	16.4	72.7

3.1.2 Development & Application of Validation Procedures for Existing Biomass Equations

A review of the literature identified two primary sources for crown biomass equations used in the interior northwest: Brown (1978) and Jenkins et al. (2003). The DBH-based equations for total crown mass (M) from these publications have been widely applied across the region and were thus selected for the development and application of equation validation methods. The destructively sampled biomass data collected as part of this study were used for validation.

An equivalence testing framework was adopted in the development of the equation validation procedures. Applying this framework, existing crown biomass equations were not presumed *a priori* to provide unbiased predictions of biomass. Instead, the working hypothesis was that an equation's prediction for a given DBH deviated appreciably from the mean crown biomass of a species at that DBH. Relative to a classical hypothesis testing framework, this equivalence testing framework shifts the burden of evidence such that establishing the goodness-of-fit of an existing equation requires the detection of a correspondence (within a certain tolerance) of the equation's predictions with the observed trends in crown biomass.

The latter form of correspondence was inferred using a double-one-sided (DOS) equivalence testing procedure (Wellak 2010) generalized for application across the DBH range of each species. To reject a general hypothesis of inequivalence, a DOS test requires that a confidence interval for the parameter of interest be completely contained within a tolerance region surrounding the postulated value for that parameter. In the present application, the parameter of interest is mean crown biomass at a given DBH, denoted symbolically by $\mu_{M|DBH}$, and its postulated value is the DBH-based prediction $\tilde{\mu}_{M|DBH}$ given by one of the existing biomass equations. Although the true value of $\mu_{M|DBH}$ for a given species and DBH is unknown, pointwise interval estimates can be obtained from the sample data for a specified confidence level. A standard DOS test at a significance level of α could then be evaluated by constructing a symmetric tolerance region around $\tilde{\mu}_{M|DBH}$ for a fixed percentage tolerance P (e.g., computing upper and lower tolerance bounds of (100-P) $\times$ $\tilde{\mu}_{M|DBH}$ and P $\times$ $\tilde{\mu}_{M|DBH}$) and then determining whether this region completely enveloped the sample-based (1-2α)$\times$100% confidence interval for $\mu_{M|DBH}$. However, the equation validation procedure developed in this study does not focus

on testing for equivalence at a given tolerance level. Instead, it is focused on determining the minimum percent tolerance (P_{min}) at a given DBH that an investigator must bear in order for the tolerance interval around $\tilde{\mu}_{M|DBH}$ to subsume the sample-based confidence interval for $\mu_{M|DBH}$, leading to a rejection of the working hypothesis of inequivalence.

To apply the validation methodology, confidence intervals for mean crown biomass conditional on DBH were estimated from the sample data using a nonparametric bootstrapping procedure. First, the relationship between total crown mass of a given species and tree DBH was described using a cubic smoothing spline. This specification allowed for a highly flexible definition of the functional form relating DBH to crown mass. Moreover, it allowed for smoothed estimates of mean crown biomass across the sampled range of DBH, not only at the observed tree sizes. The degrees of freedom of the smoothing splines were selected by minimizing mean squared prediction error over 10-fold cross-validation. To account for non-constant variance, residual deviation around the smoothing splines was described using an exponential function of DBH that was fit simultaneously with the spline coefficients via Gaussian maximum likelihood using the nlme package in R (Pinheiro et al. 2013; R Development Core Team 2008). This cross-validated fitting procedure was then replicated across 10000 bootstrap samples for each species, and pointwise percentile-based 80% confidence intervals for $\mu_{M|DBH}$ were obtained from the bootstrapped estimates.

Predicted crown biomass from the DBH-based equations of Brown (1978) and Jenkins et al. (2003) were then compared to the confidence intervals obtained at 0.25 cm increments of DBH. The minimum percent tolerance P_{min} at each DBH was calculated as the maximum deviation of the equation-predicted crown biomass from the two endpoints of the corresponding 80% confidence interval. Thus, P_{min} for a given DBH represents the minimum percent tolerance (for a symmetric tolerance region) that must be conceded in order to conclude from the sample in hand that the published equation does not systematically diverge from the true mean crown biomass at the 10% significance level.

3.1.3 Development of New Crown Biomass Equations

To develop new crown biomass equations for the 7 species of primary interest, the biomass data collected as part of this study were combined with the crown biomass data collected and published by Brown (1978). This was done to enhance the size and geographic distribution of the sample (particularly in the larger DBH classes; see Table 3-2) and because initial graphical analyses suggested consistent H:DBH and M:DBH allometries across the two data sets. Also, the data published by Brown separated the crown into similar biomass components. One exception was Brown's classification of the tree tip as a portion of stem mass (the present study treated the tree tip as a branch within the crown). Fortunately, Brown (1978) provided tip dimensions and reported tip biomass models that allowed for this typically modest component of biomass to be estimated and added to the published crown totals.

Table 3-2. Distribution of trees used in crown mass equation development; samples derive from trees measured as part of this study and from data published in Brown (1978).

Species	Num. trees	Num. stands	Mean DBH (cm)	Mean H (m)	Mean CL (m)	Mean M (kg)
DF	79	28	26.9	16.8	11.1	127.2
WL	46	14	22.6	17.7	11.3	38.8
PP	84	18	27.9	17.1	10.7	106.2
PL	43	17	23.4	18.2	8.5	58.0
GF	67	18	17.5	13.6	11.8	82.6
SF	52	19	18.8	13.5	11.6	56.4
ES	43	17	20.5	14.4	11.5	90.8

Variations in total crown mass were described using models of the general allometric form

[1] $$M_i = \underline{b}_0 X_{1i}^{b_{X_1}} X_{2i}^{b_{X_2}} \cdots X_{pi}^{b_{X_p}} + e_i$$

where the X_{ki} ($k = 1,2,\ldots,p$) are predictor variables for the i^{th} tree; $\underline{b}_0$ and the b_k are coefficients estimated from the data; and the e_i are tree-level residuals. In addition, extensions of this equation form were considered to allow for interactions among the predictors. Specifically, re-expressing equation [1] in compact exponential form,

$$M_i = \exp[b_0 + \Sigma_k b_{X_k} \ln(X_{ki})] + e_i$$

where $b_0 = \ln(\underline{b}_0)$, the extended models incorporating interaction terms took the form

[2] $$M_i = \exp[b_0 + \Sigma_k b_{X_k} \ln(X_{ki}) + \Sigma_k \Sigma_{k'} b_{X_k \times X_{k'}} \ln(X_{ki}) \ln(X_{k'i})] + e_i$$

Models forms [1] and [2] allow for the conditioning effects of multiple predictor variables in a flexible mathematical form, accommodating both convex and concave marginal response functions.

Variables used as predictors in [1] and [2] were limited to those commonly collected in forest inventory programs, with interest centering on the joint effects of DBH, H, and CL. DBH has consistently been reported as one of the strongest predictors of crown biomass (Affleck et al. 2012) and, from a biophysical standpoint, has important indirect implications for potential biomass by regulating rates of hydraulic conductivity and limiting overall mechanical support (see West et al. 1999). Past studies have reported conflicting results regarding the explanatory power of tree height after controlling for DBH, but it was included here primarily as a means of accounting for varying H:DBH ratios induced by differences in stand density and relative tree size. Both empirical associations and model specification logic suggested using the transformed height variable $\breve{H} = H - 1.37$ in place of H, thus allowing for a smooth reduction in predicted crown mass to 0 as total height approached breast height (1.37 m). Likewise, empirical trends (especially for larger trees) and allometric scaling theory (see e.g., Mäkelä & Valentine 2006) suggested inclusion of CL as a predictor, with potentially varying effects across the range of tree DBH.

Statistical estimation of crown mass models was undertaken separately by species. Estimation was carried out on the original scale (kg) and non-constant residual variation was accounted for using exponential functions of the form

$$\text{variance}(M_i) = \sigma^2 \, DBH_i^{\alpha_{DBH}} \, \check{H}_i^{\alpha_{\check{H}}} \, CL_i^{\alpha_{CL}}$$

where σ and α**.** are species-specific parameters. The parameters in the variance function were estimated simultaneously with the coefficients of [1] or [2] using Gaussian restricted maximum likelihood routines in the R package nlme (Pinheiro et al. 2013; R Development Core Team 2008).

Initial selection of crown mass models was based on 10-fold cross-validation and the computation of the following bias, mean squared error (mse), and finite-sample corrected AICC statistics from the out-of-sample data:

$$\text{bias} = \frac{\sum_i (M_i - \hat{M}_{-i}) \, \hat{v}_{-i}^{-½}}{\sum_i \hat{v}_{-i}^{-½}}$$

$$\text{mse} = \frac{\sum_i (M_i - \hat{M}_{-i})^2 \, \hat{v}_{-i}^{-1}}{\sum_i \hat{v}_{-i}^{-1}}$$

$$\text{AICC} = \sum_i \left[\ln(2\pi) + \ln(\hat{v}_{-i}) + (M_i - \hat{M}_{-i})^2 \, \hat{v}_{-i}^{-1} \right] + 2k + \frac{2k(k+1)}{n-k-1}$$

where $\hat{M}_{-i}$ is the predicted crown mass for tree i and $\hat{v}_{-i}$ is the predicted variance for tree i, with the subtraction notation indicating that both predictions are made from a model calibration that does not utilize the data from tree i; and k is the total number of estimated parameters in the model. Based on these statistics, the top three models for each species were identified. Residual diagnostics were then undertaken for these top three models. Any fitted model exhibiting evident bias within the ranges of the predictors (or within the ranges of other variables such as elevation and stand identity) were discarded. Final model selection was based minimum AICC, calculated after fitting the remaining candidate models to the full data set.

3.2 Tree Crown Terrestrial Laser Scanning & Analysis

3.2.1 Data Collection Methodology

Field Methods

Three Rocky Mountain conifer species Douglas-fir (DF), ponderosa pine (PP), and subalpine fir (SF) were sampled on 15 study sites in eastern Washington, northern Idaho and western Montana to coincide with destructive biomass sampling efforts (Fig. 3-3, Table 3-3). Stands were chosen to represent a variety of elevations, tree densities and site conditions; stand selection was constrained by landowner permission to fell trees.

Multiple trees were sampled at each site. DF and PP were most often sampled from mixed conifer stands comprised of varying balances of DF, PP, PL, WL, and others. SF was sampled

from stands comprised of SF, ES, GF and others. Sites ranged in elevation from 700 –1900 m: DF was sampled at sites between 700 – 1850 m, PP at sites between 950 – 1850 m, and SF at sites between 1350 – 1900 m. Stands ranged in basal area (measured around each sample tree) from 4.6 – 68.9 m^2/ha: DF sample sites ranged between 4.6 – 34.4 m^2/ha, PIPO sample sites ranged between 2.3 – 36.7 m^2/ha, and SAF sample sites ranged between 9.2 – 68.9 m^2/ha.

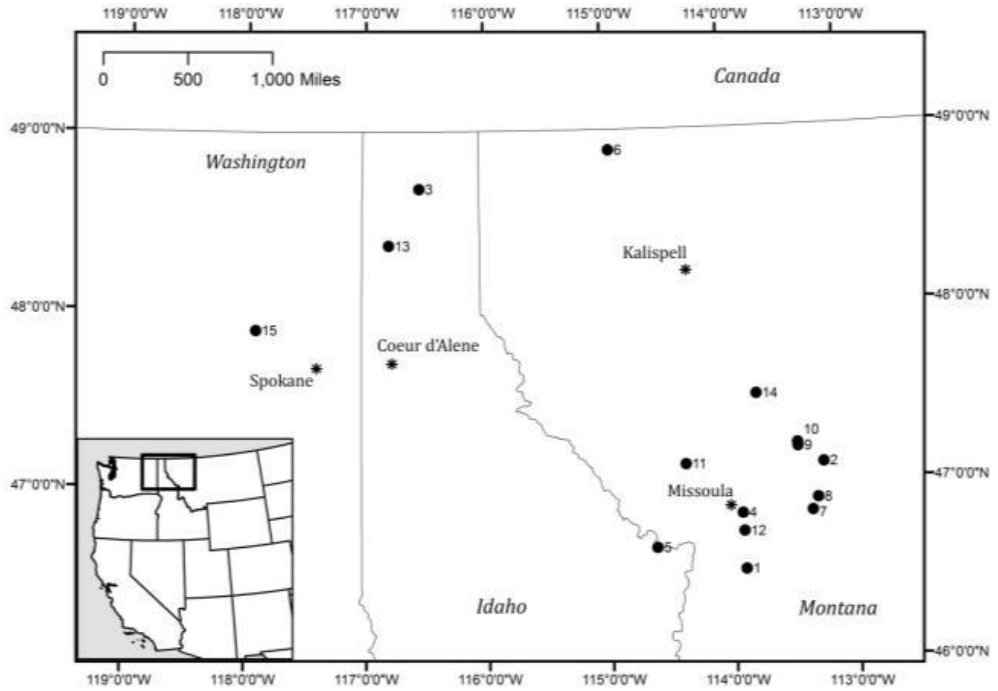

Figure 3-3. Laser scanning locations across eastern WA, northern ID and western MT. Numerical labels correspond to site details in Table 3-3.

Tree Selection

Although the stands chosen were also those sampled by as part of the destructive biomass sampling efforts, the individual trees selected had incomplete overlap. Some of the trees selected for destructive sampling were also sampled by TLS, but at each site additional trees were also scanned. The trees sampled using both methods can be used in further work to link laser return data to biomass measures. In order to sample a large number of trees across many species, trees were scanned from one perspective only. Although this provided limited information about any one tree, together, many tree scans were able to capture within species variability across size classes and geographic distributions.

Laser Scanning

Trees were scanned using an Optech ILRIS 36D HD discrete return, time-of-flight terrestrial laser scanner. The laser was mounted on a pan-tilt base atop a level tripod (Fig. 3-4). The laser records position and intensity (x, y, z, i) for each return. Trees were scanned with a spot-

spacing of approximately 4mm (3.6-5.6mm, median 3.9mm). The scanner was positioned at distances ranging from 8.2-54.9m from the target with a median distance of 23.28m. Although constant range was desired, viewshed constraints resulted in fifty-four percent of the scans completed at ranges of 15-30m, 16% at ranges < 15m and 30% at ranges >30m.

Table 3-3. Laser scanning location information: name, sampled species, location and elevation.

Site	Species Sampled	UTM Zone	Easting (m)	Northing (m)	Elevation (m)
1. Ambrose Saddle	DF, PP, SF	12	277750	5154750	1800
2. Bandy	DF, PP, SF	12	330650	5218450	1350
3. Bonner's Ferry	PP, SF	11	532930	5391612	1500
4. Deer Creek	PP	12	277950	5189800	1300
5. Granite Pass	SF	11	682250	5168250	1900
6. Kootenai	DF, PP	11	650650	5416450	1000
7. Lubrecht Garnet	DF, PP	12	321779	5188647	1850
8. Lubrecht Section 1	SF	12	325599	5196356	1900
9. Lubrecht Stinkwater	SF	12	316750	5192250	1550
10. Morrell Creek	DF, PP	11	315109	5231482	1350
11. Nine Mile	DF, PP	11	699970	5220532	1400
12. Plant Creek	DF	11	278151	5178450	1300
13. Priest River	PP	11	514050	5356150	950
14. Swan-hemlock	DF	12	291614	5263745	1200
15. Wellpinint - Tomine	DF	11	431013	5303639	700

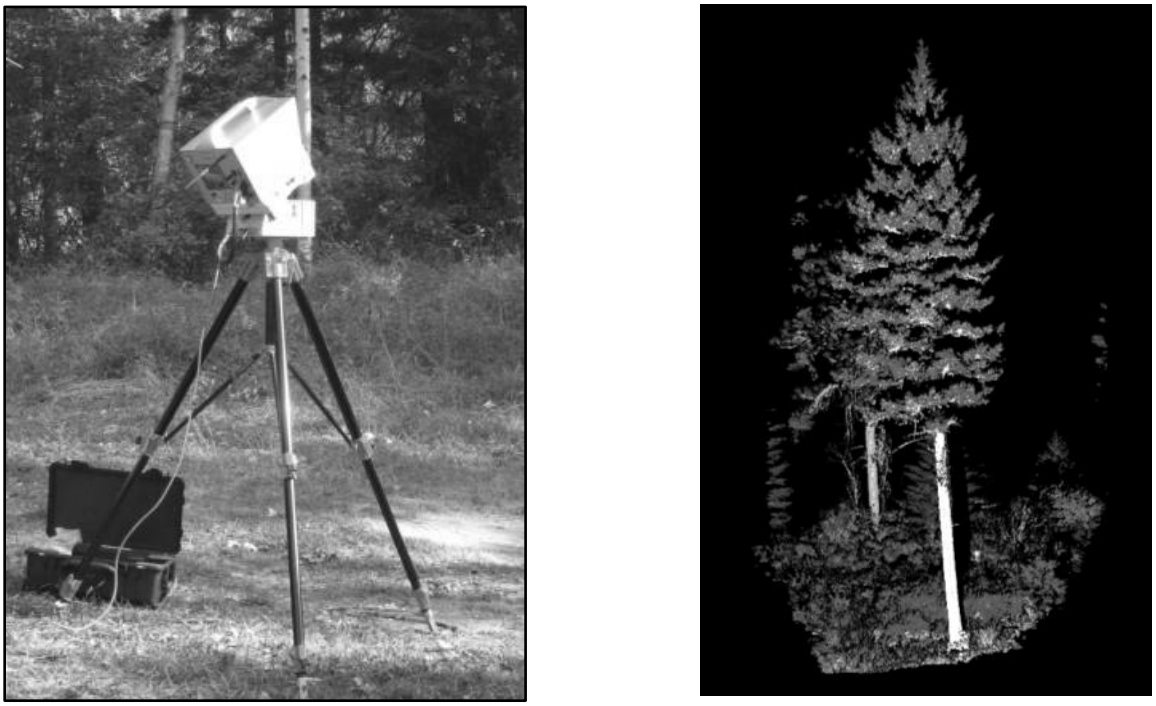

Figure 3-4. Optech laser scanner on right. Single unmerged tree scan on left.

Data Processing

Raw scan data were parsed using Optech software to text files. Overlapping bottom and top scans were aligned in Innovmetric's Polyworks V11.0.1 IMAlign. The tree of interest was isolated from each point cloud using a semi-automated process in which the user could accept or visually modify by moving within the scan.

When the base of the tree was correctly identified in XYZ space, the remainder of the bole was delineated using a process of modifying/correcting a series of ascending bole centroids. Based on proximity to the corrected bole, a line of demarcation in XZ and YZ spaces (i.e. front view and side view) was created to separate points associated with the tree of interest from the surrounding point cloud. In the YZ (side) view, laser returns behind the bole (away from the laser) were excluded from the remainder of the point cloud. After isolation, the point cloud consisted of just the points from the half of the tree of interest that was closest to the scanner.

3.2.2 Predicting Crown Shape & Volume

Width Percentiles

Crown profiles were generated from 2D simplifications of the 3D point cloud. The Z coordinate of each return in the preprocessed point cloud was retained. However, the X and Y coordinates of each return were combined into one value that described the horizontal Euclidean distance between that return and the bole centroid. This essentially "folded" the point cloud through a vertical rotation using the center of the bole as the axis, resulting in a 2D point distribution. In the new XY space, the center of the bole was the origin: the x-axis measured horizontal distance from the bole and the y-axis measured height above ground.

In 0.25 m height increments, the distribution of returns in X space was used to calculate cumulative width distribution percentiles for each height bin. Following the points delineating a given percentile (e.g. the 50th, 95th, etc.) vertically through each height increment yielded a profile for that percentile (Fig. 3-5). Width percentiles were generated using code executed in Interactive Data Language (IDL); all other crown profile analysis was completed in R (R Development Core Team 2008).

Crown Delineation and Rescaling

The LiDAR crown base height (LBH) was defined as the lowest height at which one-half the maximum width of the 95th width percentile was reached. Thus, if the maximum width of the 95th width percentile was 4.2m, the height where the 95th width percentile was 2.1m was used as the crown base. The calculated metric was evaluated relative to the field measures of crown base height (CBH) and height to live crown (HLC) (USDA Forest Service 2009).

For every tree, the retained crown 95th width percentile points were vertically rescaled between zero and one to allow comparisons between trees of different crown lengths. The width values were rescaled proportionate to original crown length for each tree by dividing

each x coordinate (representing the crown width as the distance from bole) by the crown length as calculated above. Thus, the crown percentiles were both scalable (because width was tied to height) and comparable between trees of different original sizes.

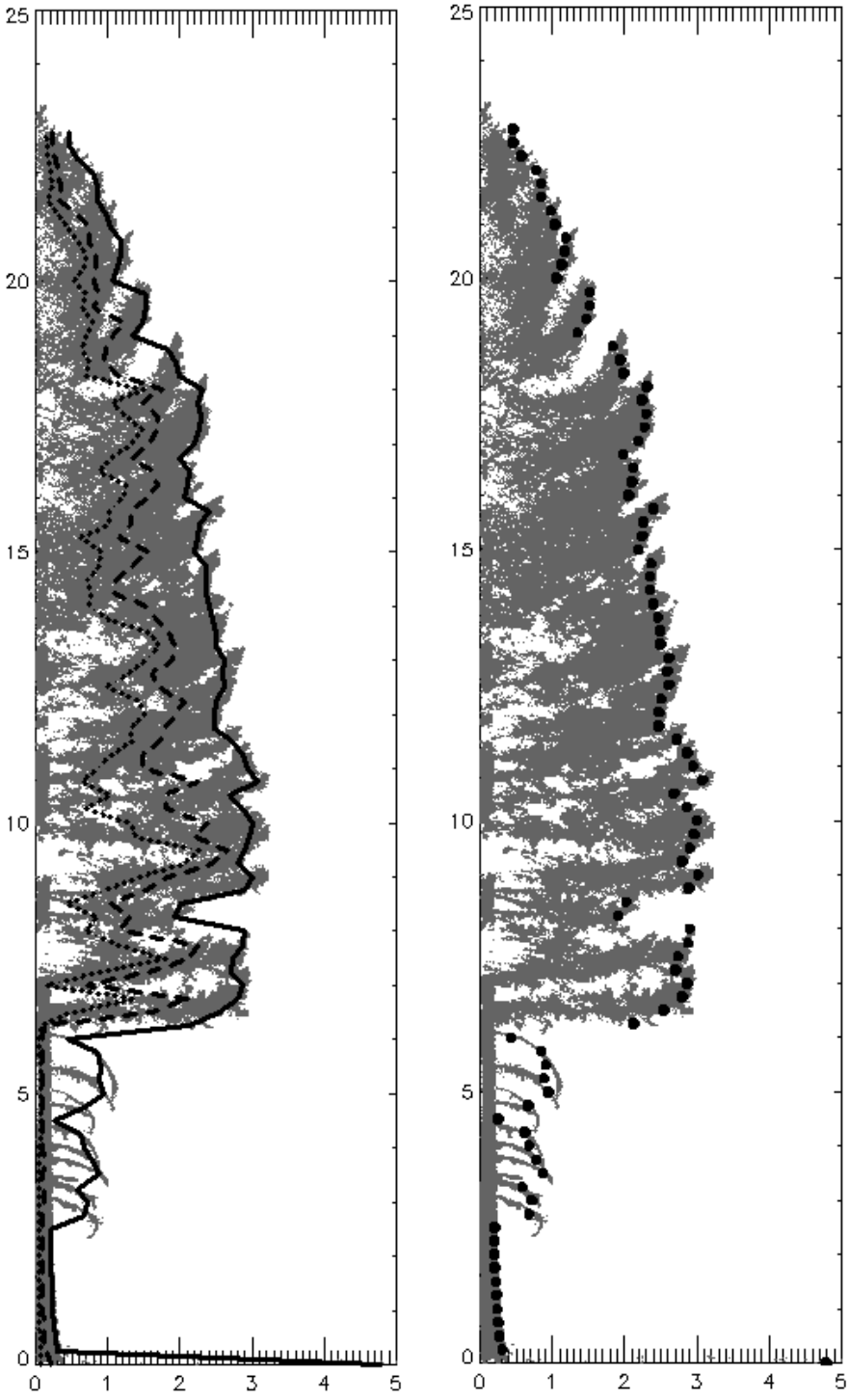

Figure 3-5. Folded DF with 25th(dotted), 50th (dashed) and 95th (solid)width percentiles. Right image shows 95th percentile displayed as points (at the 0.25m height increment bins).

Crown Modeling

After rescaling, the 95th width percentile points for all trees were aggregated into one composite representation of the 95th width percentile for each species (Fig. 3-6). Beta and Weibull curves were fit to these aggregated points to produce an aggregate crown shape for each species. Cones and cylinders were also fit to each distribution of points. Cones were shaped so that the radius of the cone at half the max height (0.5 after rescaling) was the median value of the aggregate 95th width percentile points between heights of 0.45 and 0.55. The radius of the cylinders was set using the same criteria. Those values were: DF – 0.160, PP - 0.178, SF - 0.782.

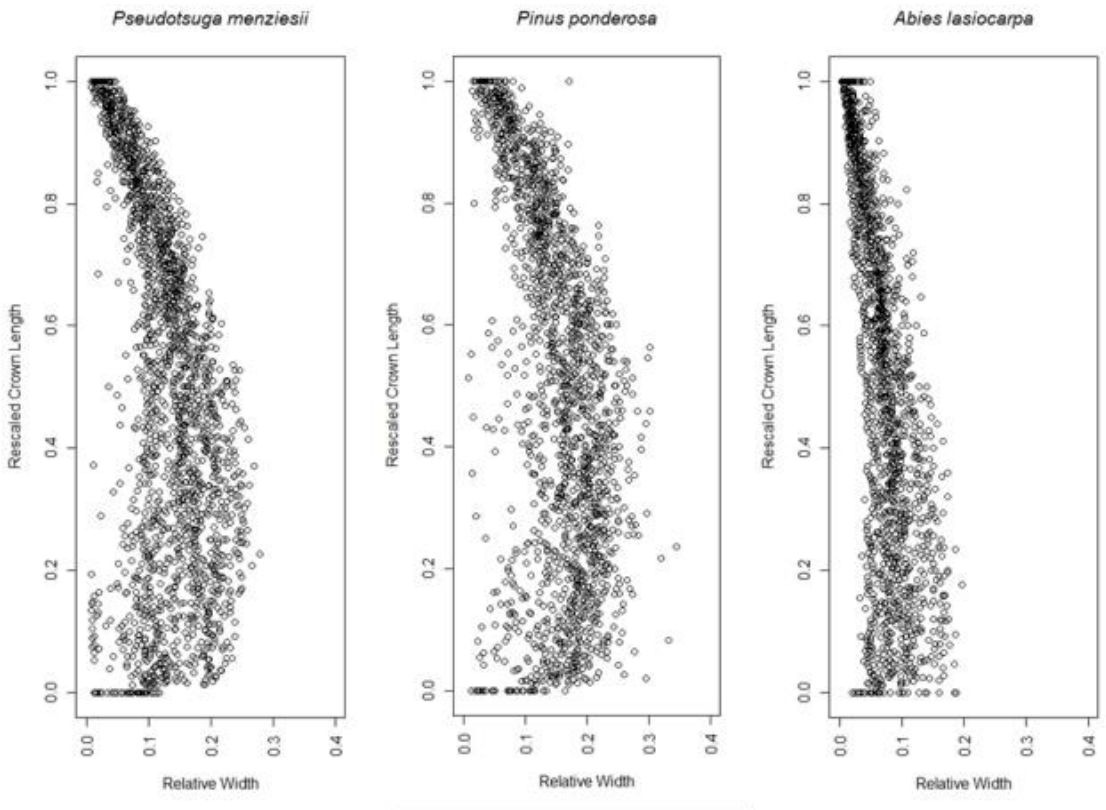

Figure 3-6. Aggregate 95th width percentile points for each species, after rescaling crown length 0-1 and the crown width relative to the crown length.

Crown Volume

The calculated average crown profile curves were used to generate volumes representing species-specific modeled tree crowns. These volumes were compared to volumes derived from the simple geometries (cones and cylinders). Crown volumes were also calculated using the curves modeled on the 95th width percentile points, plus or minus the error for that species' curve. This indicated the maximum potential volumetric variability due to curve fit issues.

Goodness of Fit Analysis

A leave-one-out cross validation was used within each species to assess curve fit using mean absolute error (MAE). Each tree's points were iteratively removed from the aggregated 95th width percentile point set, beta and Weibull curves fit to the remaining tree points, and the position of the reserved tree points were predicted from those fitted curves. MAE was calculated by subtracting the predicted width value for each reserved 95th width percentile point from the actual width value, and taking the absolute value of the result. The errors for all width percentile points were considered collectively for each species (not calculated on a per-tree basis) to determine the MAE.

3.2.3 Describing Crown Heterogeneity

The first step in characterizing the internal heterogeneity of crowns was to determine if the distribution of material departed from spatial randomness (i.e. through clustering or dispersion). Then, more detailed properties of the clusters could be described. For cluster analysis, the 3D point cloud (after pre-processing) of each tree was used – i.e. the points from the half of the tree that that was closest to the scanner. Clustering within a volume necessarily considers the native 3D point cloud (retaining the X, Y, Z, and I values), not the 2D folded data described previously for deriving crown profiles.

Ripley's L (a variant of Ripley's K) was implemented in three dimensions to assess the overall scale of clustering within each crown. Ripley's K is an index that describes departure from random patterning (Ripley 1977). For a series of radii (representing areas in 2D or volumes in 3D) around each point in a dataset, the number of other points that fall within that area/volume is counted. The average count per area/volume is compared to the average that would be expected under complete spatial randomness (CSR) (λ). Ripley's L is a version of Ripley's K where the CSR value is used for normalization. CSR becomes zero and values above zero represent spatial clustering whereas values below zero represent spatial dispersion. Ripley's K and L were calculated for each tree individually.

3.2.4 Identifying Fuel Mass by Size Class

TLS intensity data were examined to distinguish foliage and small branches (≤0.635 cm diameter; coincident with the one-hour timelag fuel size class) from larger branchwood (>0.635 cm) in DF branch specimens. Laser return density was also considered for predicting biomass by size class. Measurements were addressed across multiple ranges and scan angles. Branches were cut from trees within a single stand of second-growth DF and PP from similar crown positions and orientations. Branches were mounted on a tripod and scanned systematically from a range of distances and angles (Fig. 3-7). Each branch was then pruned to remove all 1-hour timelag fuel and scanned again. Branch material was oven-dried and weighed.

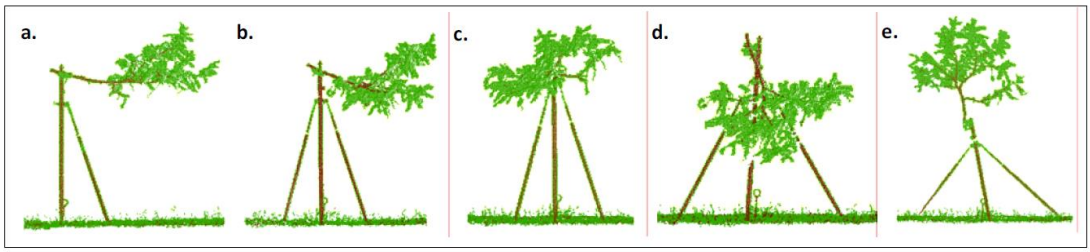

Figure 3-7. Sample branch scans at 0^{o}, 45^{o}, 90^{o}, 45^{o} up, 45^{o} down for Douglas-fir.

Nonlinear regression was used to assess the effects of range on raw intensity data. Once a suitable range correction equation was derived and applied, box-and-whisker plots were generated to compare the range-corrected result by target material (i.e., foliage, branch, Spectralon). Range-corrected intensity data from canopy fine fuels and branchwood were also assessed using box-and-whisker plots and histograms to evaluate the distinctiveness of their probability density functions. Fine fuels were distinguished from branchwood through trial and error by identifying a threshold intensity separating dim returns (fine fuels) from bright returns (branchwood). Lastly, linear regression was used to document relationships between return density and branch mass by size class, and to assess scan angle effects on mass prediction.

The threshold intensity used to distinguish fine fuels from branchwood was corroborated using two other classification schemes available in common spatial software packages; Fisher-Jenks Natural Breaks and ISODATA.

4 Key Results

4.1 Equation Validation Methodology & Results

Patterns of Variation in Total Crown Mass in Large Trees

Crown biomass increased with tree DBH at an approximately quadratic rate overall, but with species-specific and localized variations in both the form and strength of the association. Most notably, variation in crown biomass increased substantially with DBH for all species – this was evident in the scatter of sample tree data and was reflected also in the expanding widths of the pointwise confidence envelopes for mean biomass (Fig. 4-1). This variation is attributable in part to tree-level sampling error associated with the RBS procedure, but also to unaccounted for differences in tree characteristics other than DBH (e.g., variability in tree height, crown length, or branchwood density).

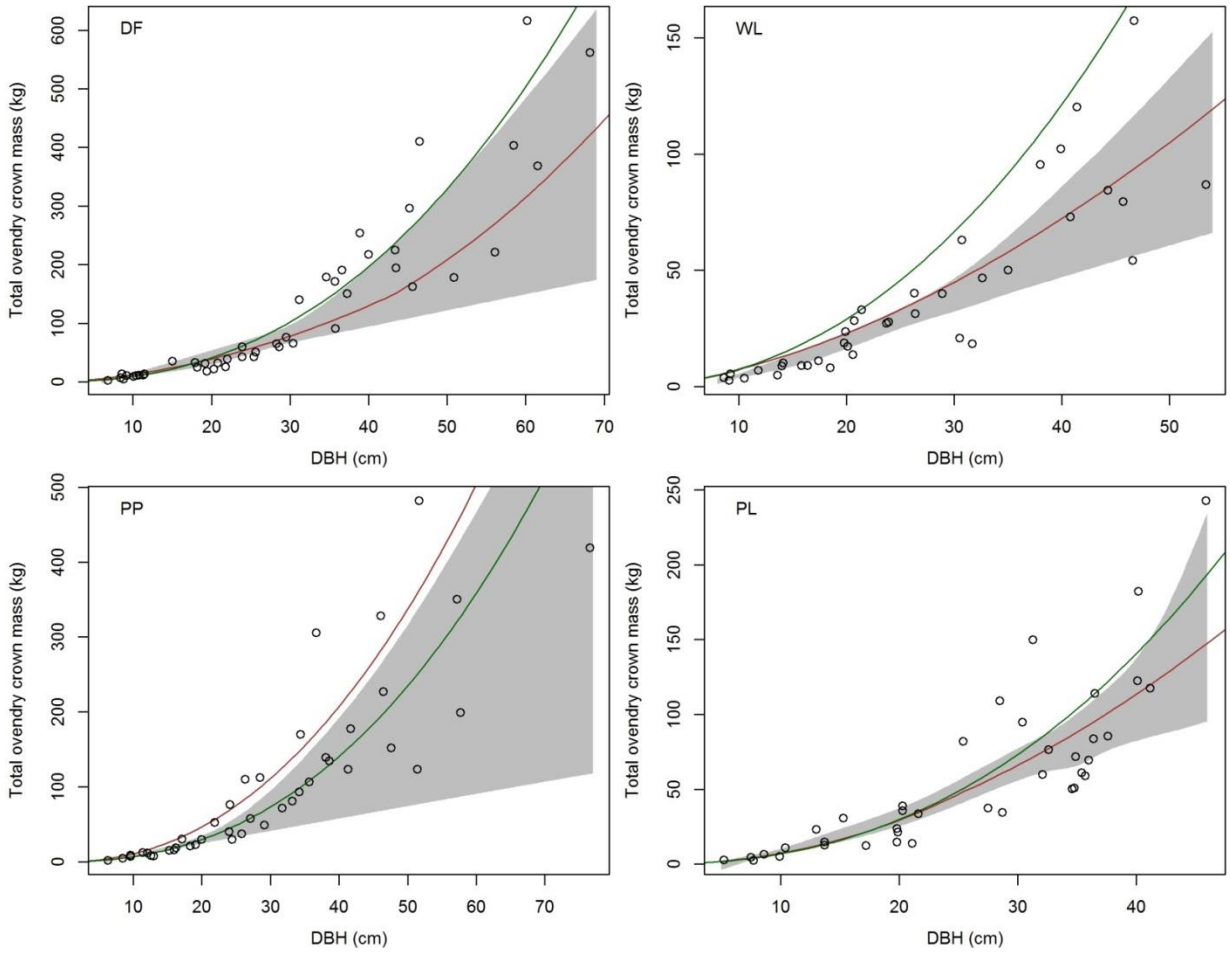

Figure 4-1 Estimated ovendry crown mass of destructively sampled trees by species as a function of DBH. Bootstrapped pointwise 80% confidence regions for mean crown mass are shaded; superimposed are DBH-based crown biomass equations from Brown (1978; red) and from Jenkins et al. (2003; green).

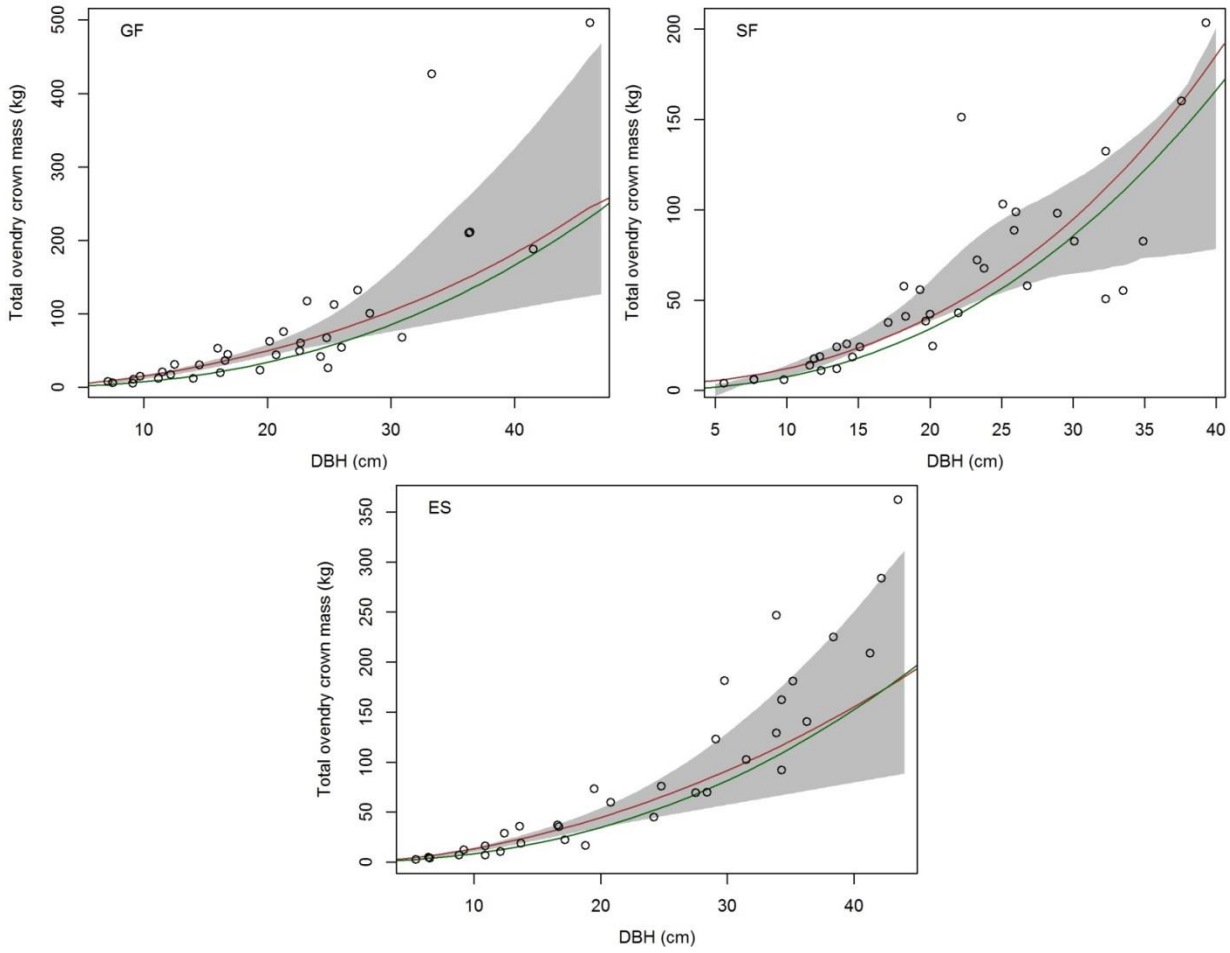

Figure 4-1 (continued).

Both tree-level sampling error and the joint effects of variation in other tree dimensions can be expected to amplify crown mass variability as tree size and DBH increase. Sampling error can be regulated through increased sampling intensity, and the RBS strategies used in this study selected an increasing numbers of branches on larger DBH trees. In contrast, variation attributable to other factors may be impossible to capture using DBH and cannot be offset by sampling intensity. Figure 4-2 shows the relationship between PP crown mass and crown length for 4 different DBH classes; it emphasizes the importance of accounting for differences in the latter variable when describing crown mass – particularly for large DBH trees. Overall, simplified characterizations of crown biomass in terms of DBH alone, coupled with relatively small sample sizes at larger DBHs, leads to appreciable uncertainty in the estimation of crown biomass for large trees (Fig. 4-1). This in turn leads to diminishing power for establishing the goodness-of-fit of novel or existing crown biomass equations.

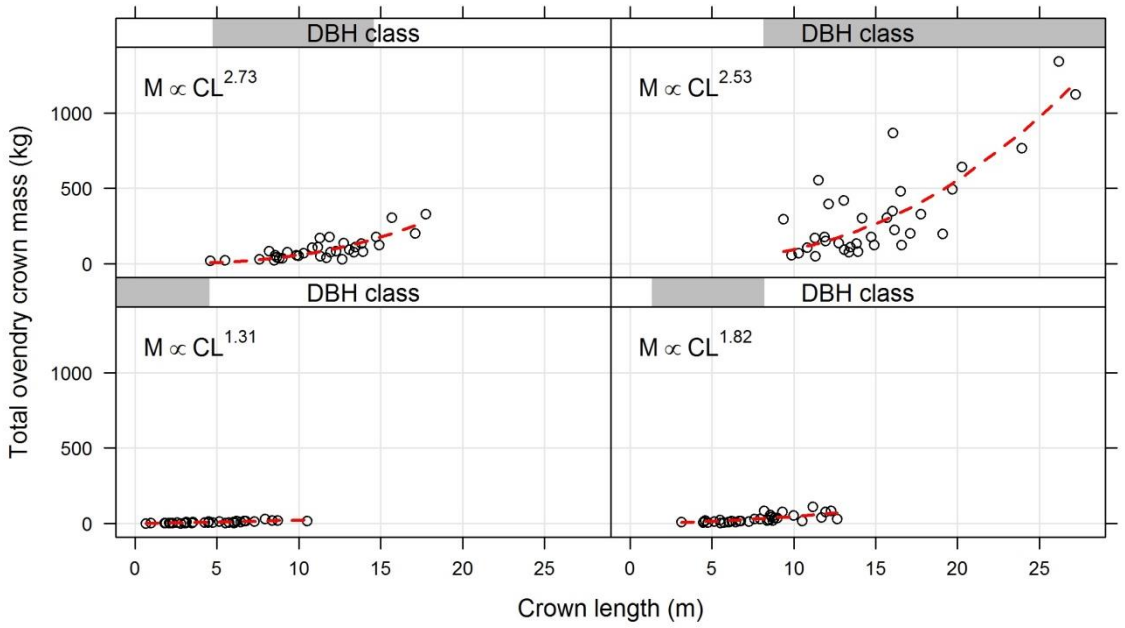

Figure 4-2. Conditioning plot of crown mass (M) against crown length (CL) for PP across 4 DBH classes.

Goodness-of-Fit of Existing Crown Biomass Equations

The DBH-based equations of Brown (1978) and of Jenkins et al. (2003) are superimposed on the scatterplots of Fig. 4-1. For some species, these equation sets produce similar predictions (e.g., ES, GF, SF) though for others the prediction differences are substantial for large DBH trees (DF, WL). It is also worth noting that, by construction, the crown biomass equations from Jenkins et al. yield identical predictions for true firs (GF and SF) and for pines (PP and PL), whereas Brown's DBH-based equations are species-specific. In the case of the Jenkins et al. equation for WL, Fig. 4-1 indicates a clear deviation of predictions from the observed data. Otherwise, the existing equations generally pass through the convex hull of the sample data.

Tracing the paths of the prediction equations relative to the 80% confidence envelopes for mean crown biomass provides a different, more complete picture. As noted above, across all species the uncertainty in mean crown biomass is appreciable for large DBH and, therefore, a considerable level of tolerance will be needed to establish goodness-of-fit at the 10% significance level – even for prediction equations that pass through the bivariate mass-DBH data distribution or within the 80% confidence envelopes. This is most evident for PP and DF where the confidence intervals grow very wide at large DBH, demanding minimum tolerances of more than 50% to reject a lack-of-fit hypothesis for either equation where DBH>40 cm (Fig. 4-3). Otherwise, for all but PP, the DBH-based equations of Brown (1978) perform better than those of Jenkins et al. (2003) in that goodness-of-fit can be established with lower minimum tolerances over greater spans of DBH. For WL, GF, and ES in particular, the goodness-of-fit of Brown's DBH-based equations can be established with these data over the mid-range of sampled DBHs at tolerances of 30% or less at the 10% significance level (Fig. 4-3). PP is the

exception in that the goodness-of-fit of the crown biomass equation of Jenkins et al. can be established with this sample over a larger range of DBH and to a tolerance of approximately 30%, though only for DBH less than 35 cm. More generally, it is impossible to conclude from these data that any of the existing DBH-based crown biomass equations are valid at tolerances of 10% or less at the 10% significance level, and in some cases not even at tolerances of 50% (e.g., Jenkins et al. equations for GF, and for most of the DBH ranges of ES and SF).

As noted, regardless of the extent of bias in the predictive equation, the power of this goodness-of-fit validation procedure declines with increasing DBH owing to increasing variability in crown biomass coupled with decreasing sample sizes. Statistical power to reject the working hypothesis of lack-of-fit is also a function of the significance level, although this can be fixed by the investigator. It is also possible to regulate the level of uncertainty by sampling more trees of large DBH. Alternatively, a parametric description of the relationship between crown mass and DBH might reduce uncertainty, though analyses of these data indicated that these relationships were inadequately captured by simple polynomial or exponential relationships. Indeed, non-parametric smoothing splines were adopted to minimize bias in the inferred mean structure, and the bootstrapping procedure was chosen to minimize lack of fit in the inferred sampling distributions.

Recognizing these caveats, it remains notable that none of the existing DBH-based equations from Brown (1978) or Jenkins et al. (2003) could be validated to within 10% at the 10% significance based on this 4-year sampling campaign. This suggests users should be judicious in the application of these equations for tree-level crown biomass estimation, particularly if data on other tree dimensions are available. At the same time, it is worth emphasizing that the equations developed by Jenkins et al. were intended primarily for national- or continental-scale applications; Jenkins et al. do not claim that these equations will yield accurate tree-level predictions for specific geographic regions such as the interior northwest. Likewise, the DBH-based equations from Brown (1978) investigated here were developed specifically for dominant/codominant trees but have been extrapolated to trees of all canopy classes. Moreover, Brown was cognizant of the limitations of strictly DBH-based equations and also reported crown biomass equations utilizing tree height and crown dimensions as predictors.

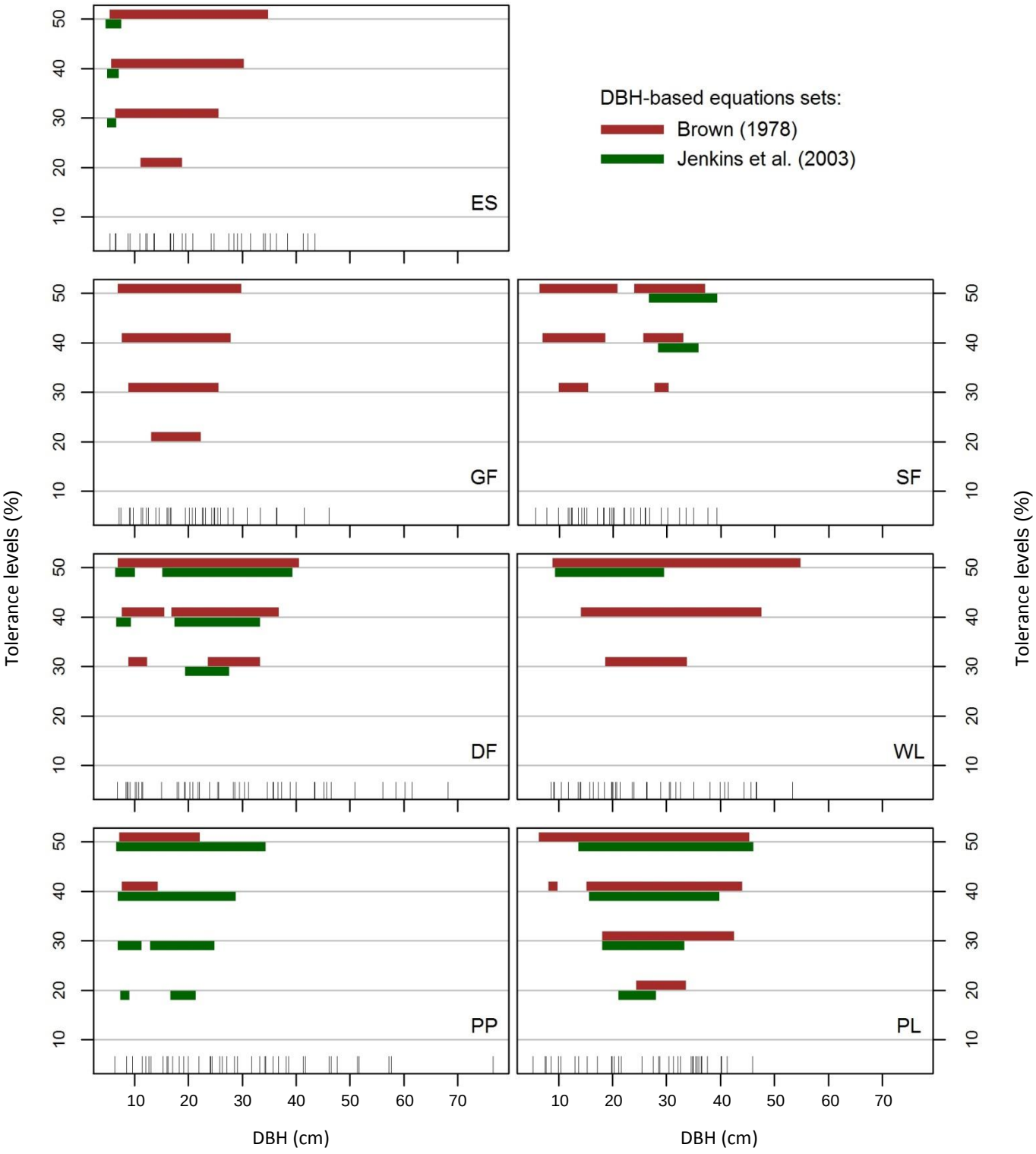

Figure 4-3. Tolerance levels at which pointwise predictions from DBH-based crown biomass equations were deemed valid at the 10% significance level. For lodgepole pine (PL), at a tolerance of ±50% the equations of Jenkins et al. (2003) are deemed valid for DBH in the range 14.5-45.25 cm; at a tolerance of ±20% the same equations are deemed valid only over the DBH range 22.0-27.25 cm.

4.2 Crown Biomass Models

Importance of Crown Length and Height as Predictors

For all 7 species, cross-validated fit statistics and residual analyses reinforced the need for crown length as a predictor of crown biomass in multivariate nonlinear regression models. The coefficients and forms of the final models are given Table 4-1. Tests indicated that DBH was the single most important predictor of crown biomass for all species. Yet for only one species (PL) did the cross-validation analyses yield a DBH-only mean structure as a candidate model, and this model form exhibited clear prediction bias when applied across the range of observed CL. Height offered additional explanatory power for all species except PL, the species for which observed heights and crown ratios were most strongly correlated. Likewise, interactions between DBH and CL added important explanatory power to the models for all species but ES.

Table 4-1. Total ovendry crown mass equation estimated coefficients (standard errors), residual standard error (se) function, and goodness-of-fit criteria ($\check{H}$ = total height – 1.37 m).

Spp	b_0	b_{DBH}	$b_{\check{H}}$	b_{CL}	$b_{DBH\times CL}$	residual se (kg)	bias (kg)	mae (kg)	R_g^2
DF	-1.775 (0.236)	2.029 (0.206)	-0.831 (0.127)	0.438 (0.156)	0.082 (0.044)	$0.052\ DBH^{0.12}CL^{2.38}$	-0.023	1.884	0.995
WL	0.158 (0.505)	0.794 (0.331)	-0.424 (0.176)	-0.651 (0.318)	0.437 (0.095)	$0.013\ DBH^{1.19}\check{H}^{0.91}$	-0.003	1.054	0.985
PP	-1.381 (0.162)	1.601 (0.152)	-0.656 (0.089)	-0.104 (0.073)	0.299 (0.031)	$0.011\ DBH^{2.23}\check{H}^{-1.55}CL^{1.95}$	0.003	0.803	0.998
PL	0.124 (0.513)	0.745 (0.245)		-0.884 (0.422)	0.465 (0.142)	$0.041\ DBH^{1.55}CL^{0.57}$	-0.006	2.663	0.953
ES	-2.599 (0.270)	2.333 (0.264)	-1.047 (0.193)	0.935 (0.277)		$0.154\ DBH^{1.52}$	0.050	4.479	0.986
GF	-0.635 (0.480)	1.236 (0.312)	-0.624 (0.224)	0.214 (0.371)	0.272 (0.088)	$0.084\ DBH^{0.88}CL^{1.16}$	-0.018	2.372	0.990
SF	-0.936 (0.514)	1.553 (0.305)	-0.938 (0.272)	0.260 (0.501)	0.248 (0.098)	$0.038\ DBH^{2.01}$	0.009	1.957	0.958

The inclusion of height and CL as predictors yields crown biomass estimates that are distinctly different than those given by the DBH-based equations of Brown (1978) and Jenkins et al. (2002). Figure 4-4 shows that the model developed for PP provides lower crown biomass estimates than Brown's DBH-based equation for large DBH and low crown ratio, but much higher estimates for large DBH and high crown ratios; the models generally agree for mid-range crown ratios (approx. 60%). Notwithstanding the preceding results emphasize the importance of validating crown biomass models using independent data, it is notable that in the development of these multivariate crown biomass models the cross-validation analyses clearly indicated the additional explanatory power of both height and crown length dimensions. From

a biological standpoint, differences in CL or in crown ratio for a fixed DBH have clear implications for crown mass (cf. Fig. 4-2). In the analyses of these data, CL was found to have an important marginal effect on crown mass, but also an important interaction effect in conjunction with DBH for all species but ES. Height (or $\check{H}$) was also an important predictor of crown mass for all species except PL. Further analyses are needed to determine whether this contribution of height can be interpreted as a modifier of the CL predictor (i.e., implicitly expressing a crown ratio effect jointly with CL) and/or as a component of a H:DBH modifier reflecting differences in stand density.

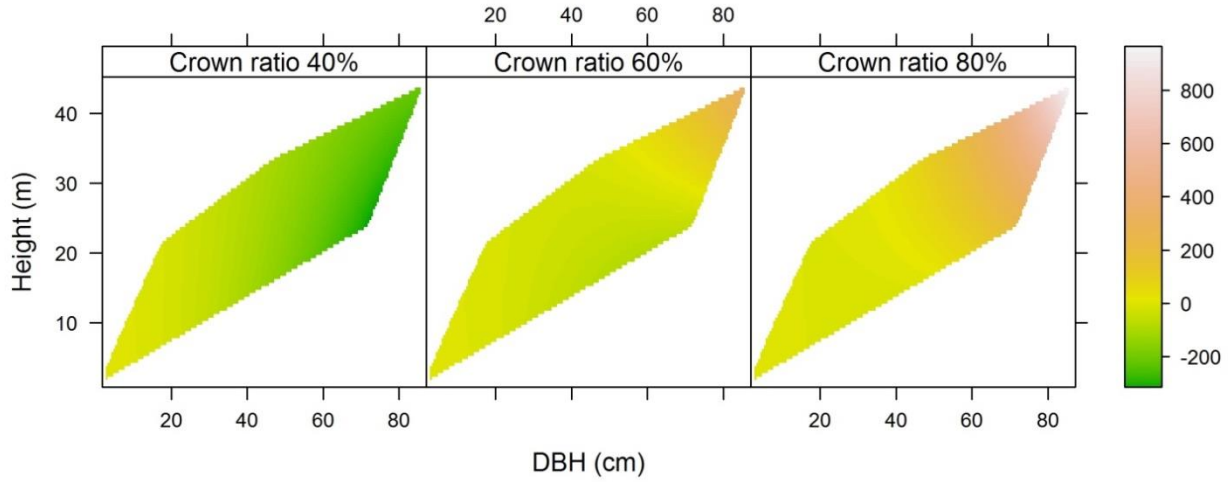

Figure 4-4. Differences between estimated PP crown biomass from the models developed in this study and the PP DBH-based equation of Brown (1978). Estimates are confined to the convex hull of the sampled distribution of height and DBH, and differences between estimates (in kg) are indicated by the color axis (negative differences in green indicate regions were Brown's equation yields larger estimates).

Species-Specificity of Crown Biomass Models

Distinct crown biomass equations were developed for each of the 7 target species (Table 4-1). However, subsequent analyses made by pooling data from GF and SF or from PP and PL indicated that the additional model complexity associated with distinct effect estimates for each species in these pairings was not offset by increased explanatory power (as measured by AICC). This was true for crown biomass models with multiple predictors as well as for models based only on DBH. It did not hold for all species pairings (e.g., distinct models for WL and DF were justified in terms of explanatory power vs. model complexity), and may not hold for crown biomass components (e.g., foliage). Nonetheless, these results indicate that pooling data from multiple species may be a cost-effective strategy for expanding the scope and distribution of crown biomass data.

4.3 Predicting Crown Shape & Volume

Laser Crown Base Delineation

Defining crown shape and volume requires a definition of crown base height. TLS produces an objective measurement of crown base height consistent with, but not identical to field measurements. In all species, LBH consistently underestimated CBH. The field-measured HLC was underestimated in trees with low crown bases and overestimated in trees with high crown bases, although this trend is weak in PP. DF and SF showed moderate correlation between calculated and field-measured crown base measures; the correlation in PP was strong. The disparity between field-measured and laser-derived crown base metric was largely due to the presence of dead branches below the live crown that were considered in the LBH, but not in the CBH or HLC. This was most common in DF, and was also seen in some trees of SF.

Better reconciliation of TLS-derived and field measured crown base height is constrained by the inability of the laser to easily distinguish live from dead branches. A metric derived solely from TLS data is desirable because it provides consistency for a measurement that can be difficult to make in the field. The LBH used was based on the presence/absence of crown material, and tended to be lower than the field definitions, which are based solely on live material. The best correlation among the measures was found in PP, which self-prunes readily and does not typically carry a large dead branch load.

Crown Profile Modeling

Folding the original 3D data based on distance to bole center is a computationally efficient way to integrate a hemisphere of data and the resultant beta and Weibull curves fit to aggregate percentile width points for each species produced excellent models (Tables 4-2, 4-3, 4-4). This approach allows prediction of a tree's crown shape from crown length alone – an easily measured or estimated metric. The 95th width percentile is an adequate descriptor of the "outer" limits of the crown, and little variation in profile shape was seen using alternate width percentiles. The volumetric changes associated with using different width percentiles were smaller than those from using simple shapes (i.e. cones or cylinders).

Table 4-2. Equation parameters for the aggregate 95th percentile points of each species.

Species	Beta	Weibull
Pseudotsuga menziesii	a = 1.2405 b = 1.5580 c = 0.1286	a = 1.4043 b = 0.6610 c = 0.1540
Pinus ponderosa	a = 1.1821 b = 1.4627 c = 0.1528	a = 1.3266 b = 0.7241 c = 0.1943
Abies lasiocarpa	a = 1.1250 b = 1.6973 c = 0.0718	a = 1.2677 b = 0.5780 c = 0.0832

Table 4-3. Mean absolute error for predictions made by the beta curve of a species for the 95th width percentile points of each tree. P-values were calculated in R.

Beta MAE	Modeled Curve Predictor Species/Shape				
Reference Species 95th Width Percentile Points	**DF**	**PP**	**SF**	**Cone**	**Cylinder**
DF	0.034 p=na	0.039 p<0.001	0.062 p<0.001	0.066 p<0.001	0.054 p<0.001
PP	0.041 p<0.001	0.035 p=na	0.084 p<0.001	0.075 p<0.001	0.052 p<0.001
SF	0.059 p<0.001	0.082 p<0.001	0.022 p=na	0.027 p<0.001	0.031 p<0.001

Table 4-4. Mean absolute error for predictions made by the Weibull curve of a species for the 95th width percentile points of each tree. P-values were calculated in R.

Weibull MAE	Modeled Curve Predictor Species/Shape				
Reference Species 95th Width Percentile Points	**DF**	**PP**	**SF**	**Cone**	**Cylinder**
DF	0.036 p=na	0.040 p<0.001	0.062 p<0.001	0.066 p<0.001	0.054 p<0.001
PP	0.043 p<0.001	0.037 p=na	0.083 p<0.001	0.075 p<0.001	0.052 p<0.001
SF	0.059 p<0.001	0.082 p<0.001	0.023 p=na	0.027 p<0.001	0.031 p<0.001

For two species (DF and PP), a scaled beta curve gave the most accurate fit to the aggregated 95th width percentile points, as measured using mean absolute error and cross-validation. For one species (SF), there was no difference in accuracy between beta and Weibull curves. In all cases, beta and Weibull curves produced significantly smaller errors than did cones or cylinders. The width percentile points of a species were best predicted by the curve calibrated for that species. For example, the species-specific curve calibrated for DF was better at predicting the 95th width percentile points for DF than any other profile, whether based on curves calibrated for other species or simple geometric solids (Fig. 4-5). In other words, profile

curves are species-specific and the loss of accuracy that results from applying one species' fitted profile to another are statistically significant. Although all of the curves were distinct, those of DF and PP were more similar to each other and to some simple geometries than they were to SF. The beta curves of DF and PP produced less error than the Weibull curves; there was no difference in accuracy between beta and Weibull curves for SF.

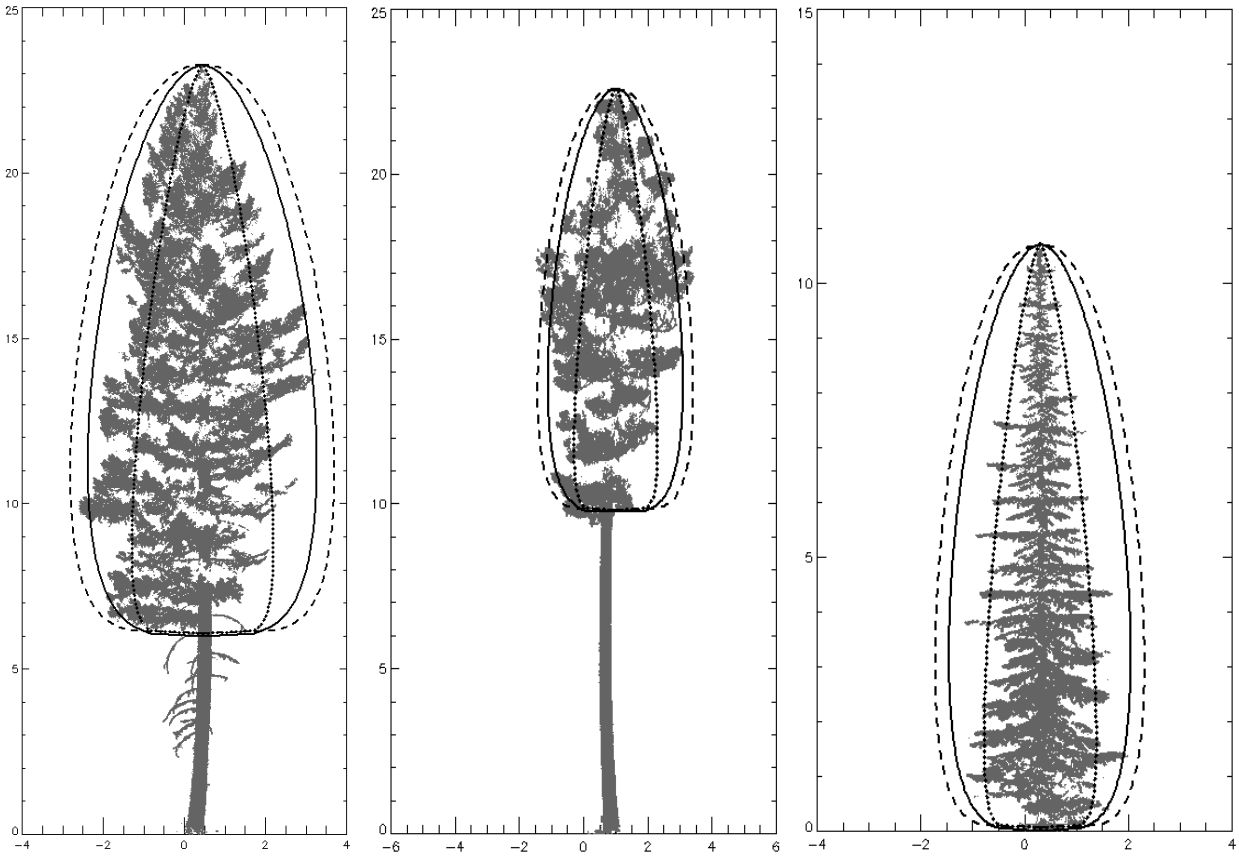

Figure 4-5. Three species beta curves on one tree of each species (height and width expressed in meters). L to R – DF, PP, SF. DF curve is solid line, PP curve is dashed line and SF curve is dotted line. Each curve was generated using species' parameters with crown length for the individual trees pictured.

The absence of relationships between model parameters and crown length, DBH, and basal area indicate that crown shape is not strongly conditioned by size and site factors, supporting the general applicability of the findings. Although the crown profile models derived from our study are likely biased to some extent toward more open-grown conditions, they nonetheless represent the best available information for the three species examined.

4.4 Describing Crown Heterogeneity

All species showed clustering occurring across larger scales (x-axis) and of greater magnitude (y-axis) in the lower portion of the crowns than the upper. The strongest clustering in DF and PP was observed at search radii of 0.0125 and 0.025, and at a radius of 0.0125 for SF

(Fig. 4-6). The search radii can be interpreted as the proportion of crown length. Thus, extrapolating values of 0.0125and 0.025 to a theoretical 20m crown produces radii of 0.25 and 0.5m at which clustering is predicted. Therefore, clusters in a 20m crown would be expected to be most prevalently sized at 0.5 – 1.0m (twice the radii) in DF and PP, and at 0.25m in SF, which suggests it is describing clustering at roughly branch scale. Because 0.0125 was the smallest radii used, branching at the individual shoot level would not be detected, except perhaps in the smallest trees.

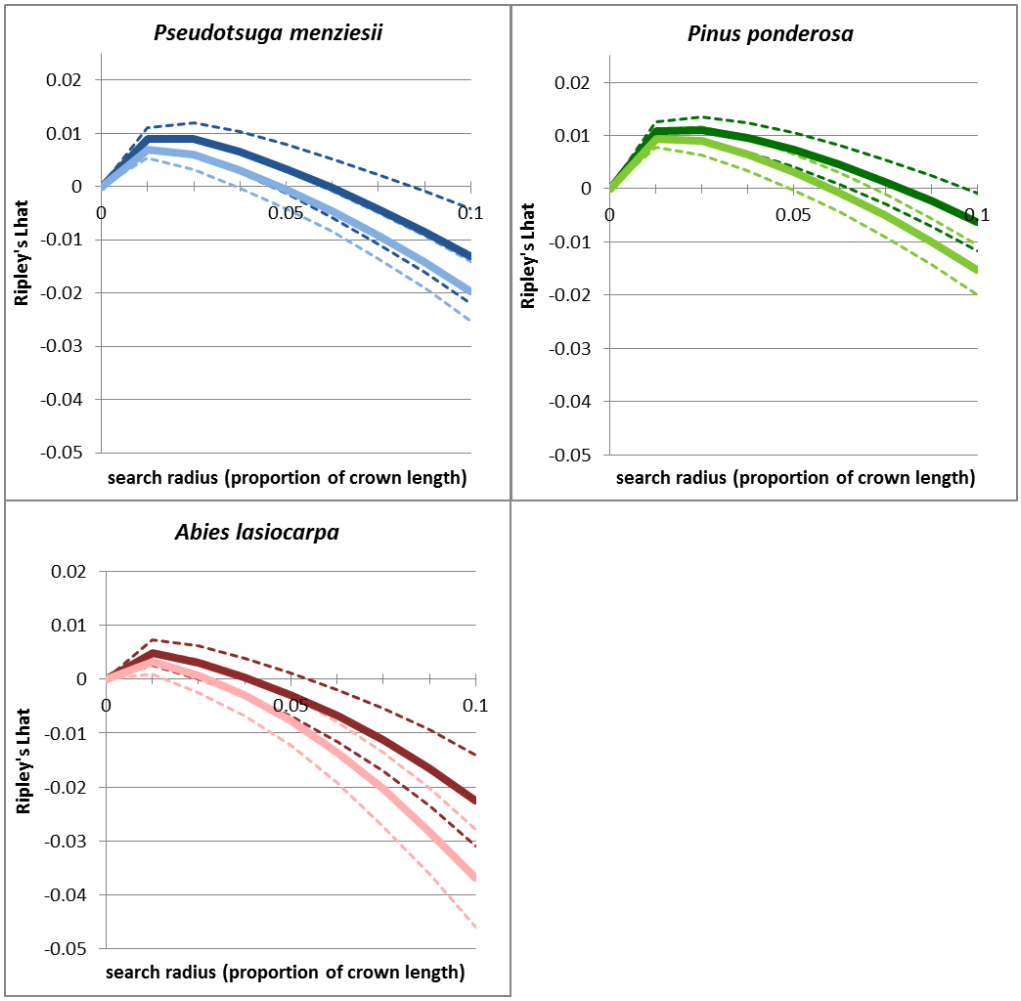

Figure 4-6. Average clustering by species. Solid lines represent the means, and dashed lines are one standard deviation above and below the mean. In each graph, the darker color represents the lower portion of the canopy and the lighter color represents the upper canopy. Because the return coordinates were rescaled relative to crown length, the x-axis of search radius distance can be interpreted as the percentage of crown length. In all cases, the y-axis is the Ripley's Lhat value and the x-axis is the search radius on the scale of the original data (here, the unitless, rescaled 0-1 crown length). Because of the rescaling of the data, the x-axis can be interpreted as the proportion of crown length (e.g. 0.05 is 5% of a 1 unit long crown).

Among species, PP showed clustering occurring over the largest scales and SF over the smallest. PP and DF had similar magnitude of clustering, while the observed clustering in SF was weaker (smaller Ripley's L values on the y-axis). Within each species, observed clustering properties between upper and lower crowns diverged as the scale of clustering increased. The average clustering in the lower crown was close to one standard deviation above the upper crown average; the average clustering in the upper crown was close to one standard deviation below the lower crown average. Worth noting is the implicit link between crown length and cluster size, where larger clusters are predicted for longer crowns. Although the Ripley's K and L functions describe the scale at which material is patterned, they do not provide explicit spatial information. Thus, no information was obtained about where in 3D space (e.g. horizontally relative to the bole or vertically in the crown) clusters were located.

4.5 Discriminating Fine Fuels from Branchwood

TLS is capable of distinguishing fine fuels (foliage and small branches (≤0.635 cm diameter, coincident with the one-hour timelag fuel size class) from branchwood (>0.635 cm diameter) in DF at a threshold of one standard deviation above mean laser return intensity. The relationship between return density and biomass is linear by fuel type for fine fuels (r^2 = 0.898; SE 22.7%) and branchwood (r^2 = 0.937; SE 28.9%), as well as for total mass (r^2 = 0.940; SE 25.5%). Intensity decays predictably as scan distances increase; however, the range-intensity relationship is best described by an exponential model rather than $1/d^2$ (where d = distance). Scan angle appears to have no systematic effect on fine fuel discrimination, but differences are observed in density-mass relationships with changing angles due to shadowing.

5 Management Implications

Crown Biomass Sampling

Destructive sampling for tree biomass is a time-consuming and expensive undertaking. There are appreciable costs associated with the field work and with the transportation, storage, disaggregation, and oven-drying of sampled materials. In assessments of individual trees, the most time-consuming element of the field work is the crown sampling. This study developed an efficient and unbiased randomized branch sampling strategy to estimate crown biomass of trees with excurrent branching patterns. The strategy capitalizes on inherent dimensional characteristics of the trees (e.g., strong associations between branch mass and branch basal area) to improve sampling efficiency without requiring prior measurement or enumeration of all branches within the crown.

Model Validation

Numerous studies have stressed the importance of biomass model validation for regional applications. This study developed a statistical validation methodology for DBH-based biomass equations. It explicitly considers the uncertainty associated with the estimation of biomass trends from sample data, can be applied across the range of an equation's input variable, and yields assessments of the percent tolerance that must be admitted in assessing an equation's goodness-of-fit. Applied using the crown biomass data collected in this study, results highlight the levels of variability in biomass given DBH, particularly for large trees. As a result, this study found that the crown biomass estimators of Jenkins et al. (2003) and the dominant/codominant tree DBH-based equations from Brown (1978) could be validated for general application across the interior northwest only for broad error tolerances, particularly for large trees. Additional study is needed to extend the validation methodology to multivariate prediction equations, such as the extended crown biomass equations of Brown (1978). Our study also highlights the need to disproportionally focus field sampling efforts on large trees in biomass model validation efforts.

Crown Biomass Models

Basic biological considerations and allometric scaling theory point to the importance of DBH as well as other tree dimensions such as crown length in conditioning overall crown biomass. Our study provides crown biomass models for the most common conifer species of the interior northwest, based on an extensive, spatially- and ecologically-distributed sample. These models incorporate DBH, tree height, and crown length effects and are calibrated from the largest crown biomass data set developed to date for the region. Model development efforts confirmed the explanatory power of crown length and tree height. They therefore suggest that, where available, the commonly measured inventory variables of tree and crown base height should be utilized in crown biomass estimation.

Terrestrial Laser Scanning

A primary goal of our TLS research is to describe the spatial arrangement of fuels within individual tree crowns sufficiently such that fire behavior modelers could produce realistic fuels data from tree lists and stand tables and use them to develop improved prescriptions for fuels treatments. From a modeling perspective, it is beneficial to be able to predict biomass from an easily obtainable measure such as DBH, predict crown shape from a single metric such as crown length, and to be able to realistically distribute predicted biomass within a predicted crown envelope. Our work addresses the first two steps for several conifer species, and begins to consider the third step.

Fire Behavior Modeling

Fire propagation in tree crowns is dependent on the spatial arrangement of flammable materials (Parsons et al. 2011). For example, simulation modeling shows that fire does not move through a crown until total foliage biomass is concentrated in volumes considerably smaller than the actual crown. One implication of this result is that the fuels inputs to fire behavior models do not map back to the fuel properties of actual trees. Our study provides improvements in the prediction of fuel mass and crown shape/volume, and suggests scales of clumpiness for three common conifer species. However, additional research is necessary to develop predictive models that describe concentrations of fuels within crowns.

Management Expectations for TLS

TLS can facilitate capturing large and detailed data sets and overcomes many of the issues associated with photographic interpretation. However, the time commitment for field work and data processing, the training required for operation of the equipment and software, and the financial outlay associated with the technology are large. At present, TLS may best be considered a specialized research instrument whose findings can be utilized to such an extent that they alleviate the need to employ it for every project. TLS may best be used to develop individual tree models for incorporation into other models or studies, rather than as a common field-sampling tool. Studies like this one can be used to exploit the capabilities of laser scanning, inform more complex models and simulations, and preclude the need to collect field data on crown structure for every project.

6 Relationship to Other Findings & Ongoing Work

In addition to the objectives originally outlined, numerous additional research questions emerged during the course of the project and remain the subject of ongoing work. This ongoing work draws on the biomass and TLS data collected in this study, as well as on complementary research projects funded by other agencies. An example of the latter is an extended tree biomass data collection and modeling effort sponsored by the USDA Forest Service's Forest Inventory and Analysis (FIA) program: this project aims to extend the biomass modeling work of the present study across all interior western states, from MT and ID south to AZ and NM. The most developed and promising avenues of ongoing work are summarized below.

Use of auxiliary information in crown sampling

The randomized branch sampling strategies employed in this study use branch and stem dimensions to select specimens for crown mass estimation. Some of the same branch and stem data could be utilized to form crown-level estimates of branch numbers and aggregate size. In turn, the latter estimates could be used to improve the precision of crown mass estimates through ratio or regression estimators. Thus, one subject of ongoing work relates to the efficiency of crown sampling and the use of various within- and across-tree calibration strategies in crown mass estimation.

Validation of multivariate prediction equations

In addition to the DBH-based equations analyzed here, Brown (1978) provides crown mass equations that utilize DBH, height, and, in some cases, crown measurements. Validation of such multivariate prediction equations is more challenging owing largely to the fact that the information from a given sample is spread more thinly when it is spread across multiple dimensions (e.g., across the DBH × height plane rather than over a simple DBH axis). Ongoing work is focused on adapting the non-parametric estimation algorithms used in this study to higher dimensions in order to extend the equivalence testing strategy to multivariate prediction equations – including the predictive equations developed as part of this study.

Extended biomass data collection & modeling

As noted above, the FIA program has funded additional tree biomass data collection and modeling efforts, and these have already supplemented the biomass data set for the interior northwest. While all aboveground components are relevant to that project, it focuses more heavily on stem biomass than does the present study. Thus, ongoing work is focused on utilizing these new data to develop compatible estimates of all components of tree biomass in the stem (bark and wood) and crown (foliage, branch size classes). The FIA-funded work will

also extend biomass data collection for many of the same species into the interior southwest, and is coordinated with data collection efforts in the Pacific Southwest and Pacific Northwest regions. As such it will provide a basis for analyses of regional variations in crown and stem biomass allometries, and of the corresponding explanatory power of climatic variables that vary widely over species ranges.

TLS & internal crown structure

Our work showed that clustering of crown material varied by species, length of crown, and height. Ongoing work is aimed at mitigating crown envelope boundary effects on the observed patterns of clustering. Additionally, we are presently focused on describing patterns and effects of laser occlusion within crowns, with an aim toward more accurate inferences of internal crown structure and associated levels of uncertainty.

7 Future Work Needed

The research questions elaborated in the previous section identify our current priorities for extending the work undertaken as part of this project. Other avenues for future work include

- Focused biomass data collection for very large trees. The present study utilized tree selection protocols that disproportionately sampled large trees, but additional sampling efforts are still needed at the large end of the DBH range. Information from very large trees is instrumental in biomass model development. Also, at the stand-level very large trees contribute disproportionately to the overall biomass per unit area so accurate estimates are needed for large trees even where these make up a small proportion of the total tree count.
- Linking branching structure and vertical biomass distributions based on felled tree data with TLS-based analyses. TLS has clear advantages over destructive sampling for describing crown profiles. Yet despite promising results regarding the discrimination of foliage and branchwood based on TLS return intensities, whether TLS alone can provide sufficient information to describe the vertical distribution of different crown materials (and the size classes of branchwood) remains an open question.
- Beyond developing crown models for additional species, future work should focus on more detailed characterization of clumping within tree crowns with the goal of developing predictive models. The main drawback to implementing Ripley's K is the lack of spatially explicit results. In short, Ripley's K can be used to identify departure from spatial randomness (clustering), but not where the clusters are located.

.

8 Literature Cited

Affleck, D.L.R., C.R. Keyes, & J.M. Goodburn (2012) Conifer crown fuel modeling: current limits and potential for improvement. *Western Journal of Applied Forestry* 27: 165-169.

Brown, J.K. (1978) Weight and density of crowns of Rocky Mountain conifers. USDA Forest Service, Intermountain Forest and Range Experiment Station Research Paper INT-197. Ogden, UT.

Gregoire, T.G. & H.T. Valentine (2008) Sampling Strategies for Natural Resources and the Environment. CRC Press: Boca Raton, FL.

Jenkins, J.C., D.C. Chojnacky, L.S. Heath, and R.A. Birdsey (2003) National-scale biomass estimators for United States tree species. *Forest Science* 49: 12-35.

Keyser, T. and F. Smith (2009) Influence of crown biomass estimators and distribution on canopy fuel characteristics in ponderosa pine stands of the Black Hills. *Forest Science* 49: 12-35.

Mäkelä, A. & H.T. Valentine (2006) Crown ratio influences allometric scaling in trees. *Ecology* 87: 2967-2972.

Parsons, R.A., W.E. Mell, & P. McCauley (2011) Linking 3D spatial models of fuels and fire: Effects of spatial heterogeneity on fire behavior. *Ecological Modeling* 222: 679-691.

Pinheiro, J., D. Bates, S. DebRoy, & D. Sarkar (2013) nlme: Linear and Nonlinear Mixed Effects Models. R package version 3.1-113.

R Development Core Team (2008). R: A language and environment for statistical computing. R Foundation for Statistical Computing, Vienna, Austria.

Ripley, B.D. (1977) Modelling spatial patterns (with discussion). *Journal of the Royal Statistical Society* 93: 172 – 212.

Schlecht, R.M. & D.L.R. Affleck (2013; under review) Branch aggregation and crown allometry control the precision of randomized branch sampling in excurrent conifer crowns. Submitted to *Canadian Journal of Forest Research*.

USDA Forest Service (2009) Field Instructions: Stand Examination. Timber Management Data Handbook FSH 2409.21h R-1 Chapter 400. USDA Forest Service, Region 1, Missoula, MT. Appendix Q.

Wellek, S. (2010) Testing Statistical Hypotheses of Equivalence and Noninferiority (2nd ed.). CRC Press: Boca Raton, FL.

West, G.B., J.H. Brown, & B.J. Enquist (1999) A general model for the structure and allometry of plan vascular systems. *Nature* 400: 664-667.

Zhou, X. & M.A. Hemstrom (2009) Estimating aboveground tree biomass on forest land in the Pacific Northwest: a comparison of approaches. USDA Forest Service, Pacific Northwest Research Station , Res. Pap. PNW-RP-584. Portland, OR. 18 p

Appendix A – Project Deliverables

Project publications, presentations, and reports are enumerated below. Alignment of these communications with proposed deliverables is detailed in Table A-1.

Conference Presentations (10)

[1] Affleck, D.L.R., J.M. Goodburn, & J.D. Shaw (2012) Strategies for assessing inter- and intra-specific variation in tree biomass in the Interior West. Forest Inventory and Analysis (FIA) Symposium 2012, Baltimore, MD, 4-6 December 2012.

[2] Ferrarese, J., E. Rowell, & C. Seielstad (2012) Species specific crown profile models from terrestrial laser scanning. Inland Northwest Growth and Yield Cooperative Annual Technical Meeting, Spokane, Washington, March 5, 2012.

[3] Ferrarese, J. & C. Seielstad (2012) Characterizing the heterogeneity of within-crown fine-fuel distribution for fire behavior simulation. Association of Fire Ecology 5th International Fire Ecology and Management Congress, Portland, OR, December 4, 2012.

[4] Turnquist, B.R. & D.L.R. Affleck (2012) Systematic Error Trends of Existing Crown Biomass Equations for the Major Commercial Conifers of the Inland Northwest. Inland Northwest Growth & Yield Cooperative Technical Meeting, 6-7 March 2012.

[5] Affleck, D.L.R. (2011) Evaluating Crown Biomass Equations for the Inland Northwest USA. Western Mensurationists' Meeting, Banff, AB, 19-21 June 2007.

[6] Affleck, D.L.R. (2011) Trends in Crown Biomass and Crown Biomass Equation Accuracy Across the Inland Northwest. Inland Northwest Growth & Yield Cooperative Technical Meeting, 4-7 March 2011.

[7] Stonesifer, C., E. Rowell & C. Seielstad (2011) Using Terrestrial Laser Scanning for biomass estimation. Inland Northwest Growth and Yield Cooperative Annual Meeting, Spokane, WA, March 4-7, 2011.

[8] Affleck, D.L.R. & B.R. Turnquist (2010) Revisiting Tree Biomass Equations for the Inland Northwest. Inland Northwest Growth & Yield Cooperative Technical Meeting, 4-7 March 2010.

[9] Rowell, E., C. Seielstad, & J. Goodburn (2010) Advances in lidar remote sensing for forestry applications. Inland Northwest Growth and Yield Cooperative Annual Meeting, Spokane, WA, March 9, 2010.

[10] Seielstad, C.A., C. Stonesifer, E. Rowell, & L.P. Queen (2010) Deriving conifer fuel mass for crown modeling using terrestrial laser scanning. International Association of Wildland Fire 3rd Fire Behavior and Fuels Conference, Spokane, Washington, Oct. 25-29, 2010.

Conference Posters (2)

[11] Ferrarese, J., E. Rowell, & C. Seielstad (2012) Modeling the geometric space of Douglas-fir tree crowns in the northern Rocky Mountains, USA for fire behavior simulation. Silvilaser2012, Proceedings of the 12th International Conference on Lidar Applications for Assessing Forest Ecosystems, Vancouver, BC, Sept 19, 2012.

[12] Seielstad, C.A., C. Stonesifer, E. Rowell, & L.P. Queen (2010) Deriving conifer fuel mass for crown modeling using terrestrial laser scanning,. International Association of Wildland Fire 3rd Fire Behavior and Fuels Conference, Spokane, Washington, October 25-29, 2010.

Peer-Reviewed Publications (3; 2 under review)

[13] Affleck, D.L.R., C.R. Keyes, & J.M. Goodburn (2012) Conifer crown fuel modeling: current limits and potential for improvement. *Western Journal of Applied Forestry* 27: 165-169.

[14] Affleck, D.L.R. & B. Turnquist (2012) Assessing the Accuracy of Crown Biomass Equations in the Inland Northwest. In McWilliams & F.A. Roesch (eds.) Monitoring Across Borders: 2010 Joint Meeting of the Forest Inventory and Analysis (FIA) Symposium and the Southern Mensurationists. GTR-SRS-157. Asheville, NC: USDA Forest Service, Southern Research Station, pp. 247-254

[15] Ferrarese, J., C. Seielstad, & D.L.R. Affleck (2013; under review) Conifer crown profile models from terrestrial laser scanning. Submitted to *Forest Ecology and Management*.

[16] Schlecht, R.M. & D.L.R. Affleck (2013; under review) Branch aggregation and crown allometry control the precision of randomized branch sampling in excurrent conifer crowns. Submitted to *Canadian Journal of Forest Research*.

[17] Seielstad, C., C. Stonesifer, E. Rowell, & L. Queen (2011) Deriving fuel mass by size class in Douglas-fir (*Pseudotsuga menziesii*) using terrestrial laser scanning. *Remote Sensing* 3: 1691-1709.

Graduate Theses (3)

[18] Ferrarese, J. (2013) Characterizing crown structure of three Interior Northwest conifer species using terrestrial laser scanning. MSc Thesis, University of Montana, Missoula, MT. 106 pp.

[19] Turnquist, B.R. (2012) Assessment of Prediction Bias in Crown Biomass Equations for Important Conifer Species of the Inland Northwest. MSc Thesis, University of Montana, Missoula, MT.

[20] Schlecht, R.M. (2011) Application of Randomized Branch Sampling to Conifer Trees: Estimating Crown Biomass. MSc Thesis, University of Montana, Missoula, MT.

Other publications & communications (2)

[21] Affleck, D.L.R., J.M. Goodburn, & J.D. Shaw (2012) Strategies for assessing inter- and intra-specific variation in tree biomass in the Interior West. In Morin, R.S., G.C. Liknes, & C. Greg (comps.) Moving from Status to Trends: Forest Inventory and Analysis (FIA) Symposium 2012. GTR-NRS-P-105. Newtown Square, PA: US Department of Agriculture Forest Service, Northern Research Station, pp. 361-364.

[22] Affleck, D.L.R. (2011) Assessment and Development of Tree Biomass Equations for the Major Commercial Species of the Inland Northwest. University of Montana College of Forestry & Conservation, www.cfc.umt.edu/ingy/CurrentProjects/INGYBiomass.php

Table A-1. Proposed deliverables and present status; references in square brackets index the project communications listed above.

Proposed Deliverable	**Status**
Documentation of conifer biomass sampling and terrestrial laser scanning protocols (*non-refereed publication*)	**Complete** [3], [12], [16], [18], [20]
Online clearinghouse for project reports and data (*website*)	**Complete & to be updated** [22] is active and will be continuously updated as peer-reviewed manuscripts and data are published.
Report on existing equation accuracy and validity (*Masters theses*)	**Complete** [19]
Presentation of existing equation accuracy assessments at regional meetings (*conference presentations*)	**Complete** [4], [5], [6], [8], [14]
Description of vertical crown profiles and/or fuel density functions from terrestrial laser scanning (*Masters thesis*)	**Complete** [18]
Geo-referenced conifer fuels data base (*data*)	**Complete & to be published** Data collected as part of this study will be made available upon publication of peer-reviewed manuscripts.
Presentation of terrestrial laser scanning crown profiling methodology (*conference presentations*)	**Complete** [2], [3], [7], [9], [10], [11], [12], [17]
Report on species-specific crown fuels equation development (*refereed publication*)	**Manuscript in preparation** Expected completion February 2014; but see also [13], [21]
Report on vertical distribution of crown fuels: methodology and results (*refereed publication*)	**Manuscript under review** [15]
Parameterized computer algorithms for decision support software (*computer algorithm*)	**In preparation** To be completed upon publication of peer-reviewed manuscripts detailing crown biomass equations and vertical profiles. Expected completion August 2014.

Appendix B – Distribution of Sample Data

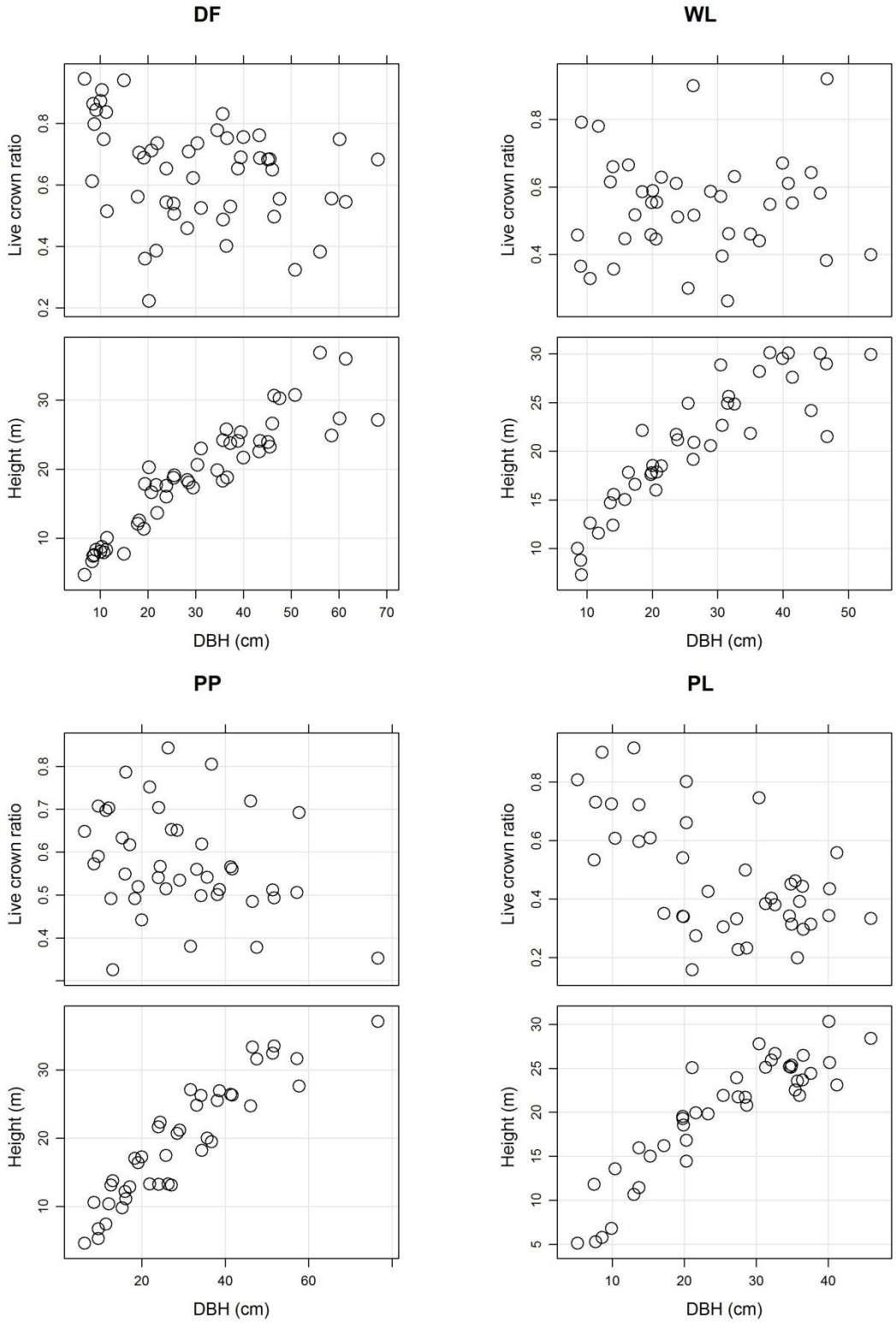

Figure B-1. Distribution of trees destructively sampled for biomass estimation by species, DBH, height, and crown ratio.

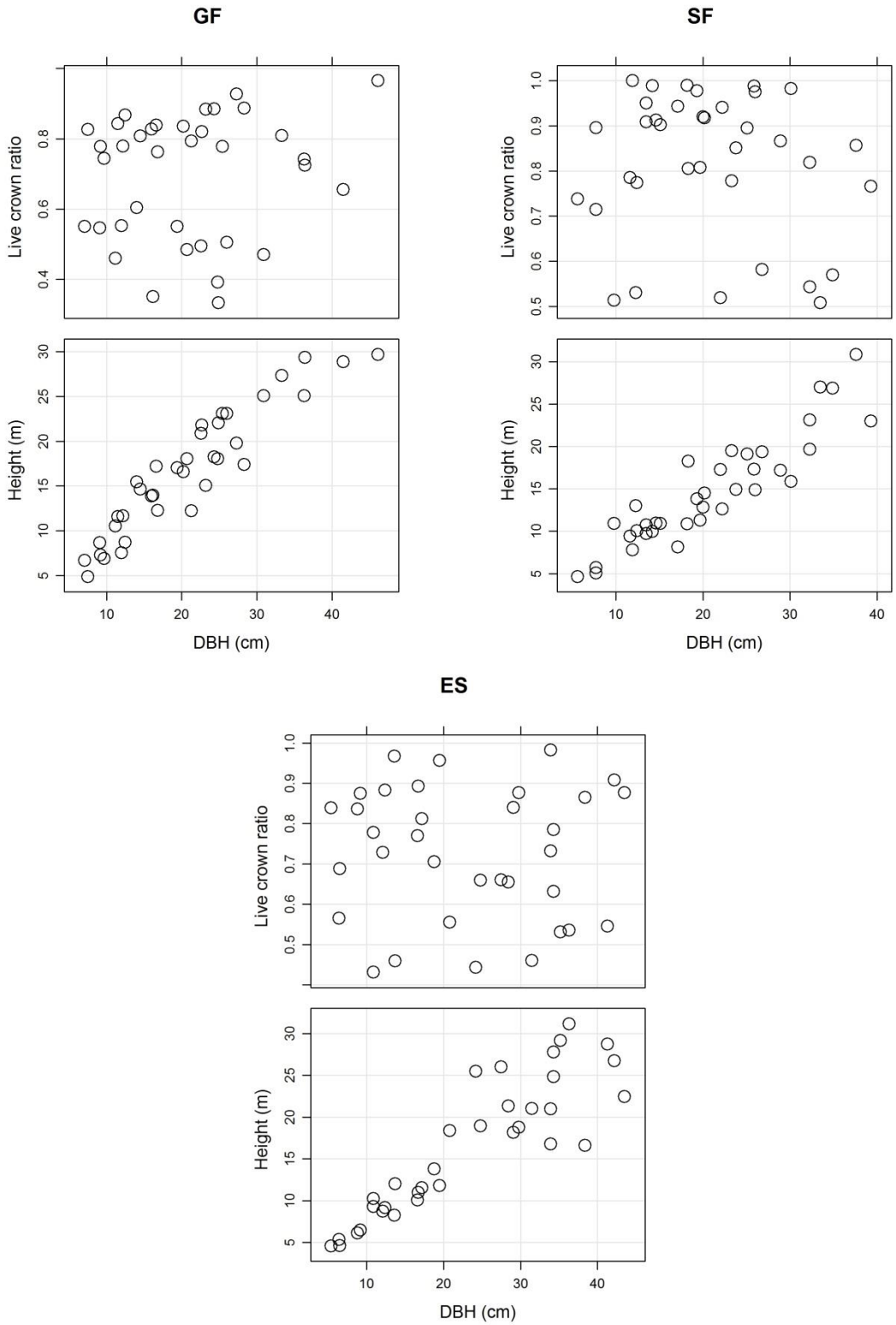

Figure B-1(continued).